PERMEABILITY OF THE CONTINENTAL CRUST: IMPLICATIONS OF GEOTHERMAL DATA AND METAMORPHIC SYSTEMS

C. E. Manning
Department of Earth and Space Science
University of California, Los Angeles

S. E. Ingebritsen
U.S. Geological Survey
Menlo Park

Abstract. In the upper crust, where hydraulic gradients are typically <1 MPa km^{-1}, advective heat transport is often effective for permeabilities $k \geq 10^{-16}$ m^2 and advective mass (solute) transport for $k \geq 10^{-20}$ m^2. Regional-scale analyses of coupled groundwater flow and heat transport in the upper crust typically infer permeabilities in the range of 10^{-17} to 10^{-14} m^2, so that heat advection is sometimes significant and solute advection should nearly always be significant. Analyses of metamorphic systems suggest that a geochemically significant level of permeability can exist to the base of the crust. In active metamorphic systems in the mid to lower crust, where vertical hydraulic gradients are likely >10 MPa km^{-1}, the mean permeabilities required to accommodate the estimated metamorphic fluid fluxes decrease from $\sim 10^{-16}$ m^2 to $\sim 10^{-18}$ m^2 between 5- and 12-km depth. Below $\sim$12 km, which broadly corresponds to the brittle-plastic transition, mean k is effectively independent of depth at $\sim 10^{-18.5 \pm 1}$ m^2. Consideration of the permeability values inferred from thermal modeling and metamorphic fluxes suggests a quasi-exponential decay of permeability with depth of $\log k \approx -3.2 \log z - 14$, where k is in meters squared and z is in kilometers. At mid to lower crustal depths this curve lies just below the threshold value for significant advection of heat. Such conditions may represent an optimum for metamorphism, allowing the maximum transport of fluid and solute mass that is possible without advective cooling.

1. INTRODUCTION

Permeability, the capacity of a material to transmit fluid, is a critical geologic parameter because migrating fluids play a fundamental role in heat and mass transfer and crustal rheology. Both hydrogeologists and geologists are actively exploring the role of subsurface fluids in such fundamental geologic processes as ore deposition, hydrocarbon maturation and migration, seismicity, and metamorphism. (For a comprehensive discussion of the role of fluids in geologic processes, see *Ingebritsen and Sanford* [1998].)

Most economically significant ore deposits exist because of the advective transport of solutes and heat by aqueous fluids. Mobilization, transport, and deposition of chemical species are all linked to fluid flow, and the thermal effects of fluid flow can explain the emplacement of certain types of ore deposits at anomalously shallow depths [*Garven and Freeze*, 1984a, b; *Bethke and Marshak*, 1990; *Garven et al*., 1993]. Similarly, the thermal effects of fluid movement may influence the position of the temperature "window" that favors the initial maturation of organic matter into hydrocarbons [e.g., *Person et al*., 1995], and hydrodynamic forces influence patterns of migration toward reservoirs where hydrocarbons are concentrated in economically significant quantities.

At generally greater depths in the crust, the occurrence and movement of fluids influences tectonism, seismicity, and metamorphism. Seminal studies of thrust faulting by *Hubbert and Rubey* [1959] and *Rubey and Hubbert* [1959] demonstrated the critical influence of fluids. In thrust faulting, part of the brittle crust is thrust over adjacent crust at a low dip angle, typically 10°–30°. Individual thrust sheets can extend over hundreds of kilometers, as in the southern Appalachian Mountains of the United States. Without consideration of fluid pressure effects, there is no satisfactory mechanical explanation for the low-angle thrusting and/or sliding of such large, thin, relatively intact sheets of rock; their strength is insufficient to withstand the required force [*Smoluchowski*, 1909]. However, *Hubbert and Rubey* [1959] showed that given elevated fluid pressures, very large blocks can slide down arbitrarily small slopes. More recently, it has been recognized that the fluid pressure regime likely controls the behavior of great transform faults where crustal plates slide past one another, such as the San Andreas fault of California [e.g., *Irwin and Barnes*, 1975; *Byerlee*, 1990, 1993; *Rice*, 1992]. In addition, metamorphism at any depth in the crust, like ore deposition, generally involves a gain, loss, and/or exchange of chemical constituents via a fluid phase. Further, most metamorphic reactions involve dehydra-

Reviews of Geophysics, 37, 1 / *February 1999*
pages 127–150
8755-1209/99/1998RG900002*$15.00*
Paper number 1998RG900002

tion, hydration, and/or changes in porosity, all of which influence the hydrodynamic regime. ("Porosity" refers to the percentage of the bulk rock volume that is occupied by connected or isolated interstices.)

In the standard Darcian flow model, the magnitude of fluid flow is a function of the intrinsic permeability k of the geologic medium, the fluid viscosity μ, and the pressure P and gravitational energy gradients acting on a unit volume of fluid. That is, in one dimension,

$$q_x = \left(\frac{k}{\mu}\right)\left(-\frac{\partial(P + \rho g z)}{\partial x}\right), \quad (1)$$

where ρ is fluid density, g is gravitational acceleration, z is elevation above a datum, and $\partial(P + \rho g z)/\partial x$ is the energy gradient for fluid flow along the flow path x, so that the proportionality between the instantaneous volumetric fluid flux along x (q_x) and the energy gradient is the quotient (k/μ). Numerical experiments on a wide range of geologic environments show that permeability is usually the primary control on fluid flux. This is because the measured intrinsic permeability of common geologic media varies by an almost inconceivable 16 orders of magnitude, from values as low as 10^{-23} m^2 in intact crystalline rock, intact shales, fault gouges, and halite to values as high as 10^{-7} m^2 in well-sorted gravels. Fluid viscosity and typical driving forces for fluid flow exhibit much narrower ranges of variation.

1.1. Variation of Permeability With Depth

Fluid flow occurs throughout the continental crust, from the surface to at least 30-km depth. Numerous attempts have been made to assess the range of crustal permeability and its variation with depth. Both theoretical models [e.g., *Gangi*, 1978] and laboratory results [e.g., *Morrow et al*., 1994] suggest that the permeability of fractured crystalline rocks generally decreases with increasing confining pressure or effective stress. Although *Brace* [1980, 1984] concluded that there was little evidence for depth-dependent permeability in crystalline rocks, most of his in situ data were from <500-m depth, and more recent data indicate a dependence on confining pressure that varies with rock type and the extent of weathering. Less-fractured gneissic rocks from the Black Forest of Germany show depth-dependent in situ permeability, whereas highly fractured granitic rocks from the same region do not [*Stober*, 1996]. Similarly, the laboratory-scale permeability of relatively fracture-free basalts from the deep Kola (Russia) and KTB (Germany) drill holes is sensitive to confining pressure, whereas highly fractured granodiorite gneisses from the same holes are less pressure-sensitive [*Morrow et al*., 1994]. The laboratory-scale permeability of deep drill hole core samples is generally both lower and more pressure-sensitive than the permeability of similar rocks sampled at surface outcrops [*Morrow and Lockner*, 1994]. The lack of pressure sensitivity in the outcrop samples may result from near-surface unloading and weathering, which causes near-surface fracture openings to be less uniform, and therefore less easily closed, than those at depth.

In the absence of a clear understanding of permeability variations throughout the crust, regional-scale models of groundwater flow invoke fairly arbitrary permeability-depth curves. For example, in the Dakota Sandstone, correlations between log k and porosity n and between log n and depth lead to variations in sandstone permeability of about 3 orders of magnitude over about 4 km depth. This led *Belitz and Bredehoeft* [1988] to propose $\log(\log k/k_0) \propto$ depth, where k_0 is the near-surface permeability. To represent the permeability of cross sections across the San Andreas fault in California, *Williams and Narasimhan* [1989] chose $\log k = -0.2 \times$ depth (km) $- 15$, so that permeability varied from 10^{-15} m^2 at the surface to 10^{-18} m^2 at 15-km depth, roughly matching the range of permeabilities measured in nearby boreholes in fractured (10^{-15} m^2) and intact (10^{-18} m^2) crystalline rock. Such permeability-depth relations are applicable only to the locality for which they were derived. If extrapolated to deeper active metamorphic environments, the permeability values invoked by the *Williams and Narasimhan* [1989] relation are substantially lower than those predicted for dewatering crust undergoing advective solute transport [e.g., *Bickle and McKenzie*, 1987; *Connolly and Thompson*, 1989].

1.2. Purpose and Scope of This Paper

It seems likely that in tectonically and/or thermally stable environments, permeability may diminish to vanishingly small values at depths where rock strength is low. However, numerous studies focused on more active environments have documented the existence of hydrologic systems operating over a range of scales and at all depths in the continental crust. In this paper we focus on the magnitude of permeability in these active hydrologic systems as constrained by geothermal studies and estimates of metamorphic fluid flux. We begin by briefly reviewing the nature of crustal permeability, including its heterogeneity and its time and scale dependence. We then describe simple calculations that elucidate the limiting permeabilities required for such geologically significant processes as generation of excess pore fluid pressures and advective transport of heat and solutes. Finally, these "process-limiting" limiting values of permeability are used in conjunction with geothermal and metamorphic data to obtain estimates of crustal permeability and a speculative permeability-depth curve for the hydrologically active crust (Figure 8).

2. VARIATION OF PERMEABILITY IN THE CRUST

Although the main purpose of this paper is to use geothermal and metamorphic data to assess the variation of permeability with depth in the crust, there are other sources of permeability variation that require

some discussion, including heterogeneity and anisotropy, temporal variation, and scale variation. We will argue that these factors can (and sometimes must) be ignored in analysis of the geothermal and metamorphic data.

2.1. Heterogeneity and Anisotropy

Near the Earth's surface, permeability exhibits extreme spatial variability (heterogeneity) and anisotropy, both among geologic units and within particular units. For example, permeability commonly shows 10^4-fold variation within particular ash flow tuff [*Winograd*, 1971] and soil [*Mitchell*, 1993] units. The most obvious sources of anisotropy in permeability are sedimentary and volcanic layering and fracture patterns, but foliation in metamorphic rocks also causes anisotropy; *Huenges et al*. [1997] found mean permeability parallel to foliation to be about 10 times larger than mean permeability perpendicular to foliation. In general, permeabilities parallel to planar elements tend to be much higher than the permeabilities orthogonal to them. Such anisotropies can have a large impact on heat and mass transport in convecting systems where permeability is sufficiently high [e.g., *Rosenberg and Spera*, 1990]. By solving Darcy's law for a series of stacked layers [e.g., *Maasland*, 1957] it can be shown that the equivalent vertical permeability k_z of m layers is given by the harmonic mean of the layer permeabilities, $k_z = b_t/(\sum_{i=1}^{m} b_i/k_i)$, where b_i and k_i are the thickness and permeability of the ith layer and b_t is the total thickness of the stacked layers. The equivalent horizontal permeability k_x of m layers is given by the arithmetic mean, $k_x = \sum_{i=1}^{m} k_i(b_i/b_t)$. This implies that the equivalent vertical permeability of stacked layers will tend to be controlled by the lower-permeability layers, whereas the equivalent horizontal permeability will tend to be controlled by the higher-permeability layers.

Although local heterogeneity and anisotropy are greatest near the Earth's surface, heterogeneity in permeability also exists in the middle and lower crust below the brittle-plastic transition, where it is a consequence of variations in pore network geometry within and between lithologies that arise from variations in rheology, mineral types, shape factors, and volatile contents [*Oliver*, 1996]. Almost all analyses of metamorphic fluid flow deduce that permeability varies within and between lithologies. Recent studies have noted heterogeneities within lithologies exceeding a factor of 10^2 [e.g., *Cartwright and Oliver*, 1992, 1994; *Cartwright and Weaver*, 1993; *Cartwright*, 1994; *Cartwright and Buick*, 1995; *Baumgartner et al*., 1997] and that time-integrated fluid fluxes tend to be greater along lithologic contacts than across them, implying greater permeability parallel to bedding or other lithologic boundaries [e.g., *Rumble and Spear*, 1983; *Nabelek et al*., 1984; *Ganor et al*., 1989; *Bickle and Baker*, 1990; *Cartwright and Oliver*, 1994; *Cartwright et al*., 1995; *Skelton et al*., 1995].

The anisotropy of permeability motivates a three-dimensional version of Darcy's law in which permeability appears as a second-rank tensor [e.g., *Bear*, 1972]. However, the geothermal and metamorphic system data that we examine in this paper generally permit estimation of only scalar values of permeability. The permeabilities obtained from consideration of geothermal data, which are mainly from sedimentary basins and layered volcanic rocks, usually represent some combination of flow along and across layering, although in rare instances [e.g., *Deming*, 1993] it is possible to estimate both horizontal and vertical permeability from a particular data set. The values obtained from metamorphic data likely represent the maximum value of the permeability tensor, because metamorphic flux-based permeability estimates are based mainly on flow within lithologies; mean flux (and permeability) normal to lithologic contacts is generally lower.

2.2. Temporal Variation

Because of ongoing deformation, dissolution and precipitation of minerals, and other metamorphic processes, permeability is a time-dependent property. The transient nature of permeability has long been recognized by economic geologists, who see evidence of episodic fracture creation and healing in fossil hydrothermal systems [e.g., *Titley*, 1990]. The feedbacks between transient permeability and such processes as compaction, hydraulic fracturing, poroelastic response, and dissolution-precipitation reactions have been quantitatively explored by *Walder and Nur* [1984], *Connolly and Thompson* [1989], *Nur and Walder* [1990], *Norton* [1990], *Lowell et al*. [1993, 1995], *Dutrow and Norton* [1995], and *Connolly* [1997b], among others. However, time-dependent permeabilities are rarely incorporated in quantitative analyses of fluid flow and transport.

Although time itself is not the activating factor, it is useful to consider the timescales over which various geologic processes are likely to affect permeability. Some geologic processes (e.g., hydrofracturing or earthquakes) act very rapidly, whereas others (e.g., compaction of sediments) cause a gradual evolution of permeability. The fact that earthquakes can instantaneously change permeability on a regional scale was vividly demonstrated by the M 7.1 Loma Prieta (California) earthquake of 1989; immediately after the earthquake, many streams within ~50 km of the epicenter experienced a tenfold increase in streamflow [*Rojstaczer and Wolf*, 1992]. Water-rock reactions can also cause permeability to evolve fairly rapidly: analyses of near-surface silica precipitation in hydrothermal upflow zones indicate that at high temperatures (~300°C), large (1 mm) fractures can be sealed by silica precipitation in 10^1 years [*Lowell et al*., 1993], and simulations of calcite dissolution in coastal carbonate aquifers suggest significant changes in porosity and permeability over timescales of 10^4–10^5 years [*Sanford and Konikow*, 1989]. The reduction of pore volume during sediment burial modifies permeability more slowly. For example, shale permeabilities from the U.S. Gulf Coast vary from about 10^{-18} m^2 near the

surface to about 10^{-20} m^2 at 5-km depth [*Neglia*, 1979], and the natural subsidence rate is 0.1–10 mm yr^{-1} [*Sharp and Domenico*, 1976], so we can infer that it takes perhaps 10^5–10^7 years for the permeability of a subsiding packet of shale to decrease by a factor of 10.

The permeability values that we will evaluate here, based on geothermal and metamorphic data, are averages that apply over long time periods and often over large spatial scales. The conductive thermal regime evolves slowly (e.g., over 10^4 years on a length scale of 1 km), and estimates of metamorphic permeabilities often rely on fluid flux estimates for the entire duration of active fluid flow (e.g., perhaps 10^5 years for prograde contact metamorphism). Thus the geothermal and metamorphic data provide little quantitative information on the transient variation of permeability.

2.3. Scale Variation

Values of permeability are often determined by three methods, each of which measures or infers permeability at a different volume-averaged scale. Laboratory tests measure permeability at the drill core scale, and the volume of material sampled is generally very small, almost always $\ll 1$ m^3. The volume of material sampled by in situ or well bore tests varies with the size and duration of the perturbation and with the hydraulic properties of the medium, but generally ranges from <10 m^3 (for a single-well test in a low-permeability medium) to perhaps $>10^7$ m^3 in a high-permeability medium. Larger-scale "regional" values are often inferred from the results of numerical modeling experiments. Regional permeability values inferred on this basis are applied to volumes ranging from perhaps 10^0 to $>10^3$ km^3.

On the basis of measurements and inferences at these different and often nonoverlapping scales, permeability often appears to be a scale-dependent property. The apparent scale dependence is most pronounced in crystalline rocks where permeability is provided largely by discrete fractures. For such rocks there is typically a 10^4- to 10^6-fold variation among laboratory-scale measurements of samples from a particular site [*Brace*, 1980], and the mean in situ value is typically about 10^3 higher than the mean value determined by laboratory tests [*Brace*, 1980, 1984; *Clauser*, 1992]. This is because the cores for laboratory analysis (typically ~0.1 m long) tend to come from mechanically sound (unfractured) sections of the well bore. The in situ tests sample a longer section of well bore (usually >10 m) and encounter more of the natural heterogeneity of the medium. In contrast to experience in crystalline rocks, laboratory and in situ permeability measurements on argillaceous (clay rich) rocks often agree to within an order of magnitude [*Brace*, 1980; *Neuzil*, 1994], though there are exceptions.

Crustal permeability values based on geothermal and metamorphic data are averages that apply over some spatial scale. In most cases, the applicable scale is rather large (in the case of geothermal data, the length scale is usually >100 m and often >10 km). At such large scales, permeability data from the uppermost crust show no clear scale dependence [*Clauser*, 1992].

3. USE OF GEOLOGIC OBSERVATIONS TO CONSTRAIN PERMEABILITY

Because fluid flow influences pore fluid pressures, heat transport, and solute transport, observations of pressures, temperatures, and metamorphic reaction progress can be used to constrain flow rates and/or permeabilities. In this section we use analyses of homogeneous, one-dimensional systems to estimate key "process-limiting" values of permeability; in particular, the approximate limiting values required for generation of elevated pore fluid pressures and significant advective transport of heat and solutes. Such limiting values can then be compared with geothermal and metamorphic data to obtain a first-order estimate of permeability throughout the crust.

3.1. Elevated Fluid Pressures

Elevated fluid pressures are of considerable geologic interest because they change the state of effective stress and reduce the work necessary for deformation [*Hubbert and Rubey*, 1959]. A simple one-dimensional analysis can be used to estimate the permeability required to allow generation of excess pore fluid pressures in diverse geologic settings [*Neuzil*, 1995]. In the context of standard equations of groundwater flow, fluids produced by metamorphic devolatilization or other geologic processes such as sediment compaction and oil generation may be treated as sources or sinks of fluid [*Bredehoeft and Hanshaw*, 1968]. That is, for example,

$$s_s \frac{\partial h}{\partial t} = \nabla \cdot \bar{K} \nabla h + \Gamma, \tag{2}$$

where s_s is the specific storage, or change in the volume of fluid stored in a unit volume of porous medium per unit change in hydraulic head [*Jacob*, 1940]; K is hydraulic conductivity, a lumped parameter ($K = k\rho_f g/\mu_f$) that includes the influence of both fluid (specific weight $\rho_f g$, and viscosity μ_f) and medium (k) properties on the ability to transmit fluid; h is hydraulic head [*Hubbert*, 1940]; and Γ is the source term ($L^3/(L^3T)$ or $1/T$). This formulation, in conjunction with estimates of Γ obtained from the literature [e.g., *Neuzil*, 1995] provides a basis for estimating when fluids generated by geologic processes are likely to have a significant effect on the fluid pressure distribution.

For a homogeneous, isotropic hydraulic-conductivity field, equation (2) can be written in dimensionless form as

$$\frac{\partial h_d}{\partial t_d} = \nabla^2 h_d + \Gamma_d, \tag{3}$$

where the operator ∇^2 and hydraulic head h_d have been nondimensionalized with a representative length L, dimensionless time t_d is given by Kt/s_sL^2, and the dimensionless source Γ_d is given by $\Gamma L/K$. Then, assuming conservatively that hydraulic head gradients greater than unity indicate a significant level of excess fluid pressure, it can be shown that that such gradients would be expected for a variety of domain geometries if [*Neuzil*, 1995]

$$K < |\Gamma|L. \quad (4)$$

The potential for significant effects on the fluid-pressure regime thus depends only on the strength of the fluid source, the size of the domain, and the hydraulic conductivity.

The widespread occurrence of reticulate fracture networks ("stockworks") in contact-metamorphic environments is commonly attributed to fluid pressures that temporarily exceeded the stress required for failure, leading to hydraulic fracturing of the rock mass [e.g., *Titley*, 1990]. Using equation (4) we can easily estimate the conditions under which metamorphism is likely to lead to anomalous pore fluid pressures. For example, devolatilization of a 1-km-thick layer of rock in a regional metamorphic setting ($\Gamma < 3 \times 10^{-15}$ s^{-1} [*Hanson*, 1992]) might lead to anomalous fluid pressures if the hydraulic conductivity of the layer, K, is less than 3×10^{-12} m s^{-1} (or, alternatively, if the layer were bounded above and below by comparably thick and poorly conductive layers). At a temperature of about 300°C this limiting value of hydraulic conductivity would translate to an intrinsic permeability k of the order of 10^{-19} m^2, the same value that is required for significantly elevated fluid pressures in *Hanson*'s [1997] detailed numerical analysis of regional metamorphism. In a 100-m-thick contact-metamorphic zone adjacent to an igneous intrusion, the combined effects of heating and devolatilization ($\Gamma \approx 6 \times 10^{-13}$ s^{-1} [*Palciauskas and Domenico*, 1982; *Hanson*, 1992]) might lead to anomalous pressures for wall rock $K < 6 \times 10^{-11}$ m s^{-1} or, at $T \approx 300$°C, for wall rock $k \leq 10^{-18}$ m^2. In general, it appears that the rate of fluid production by various geologic processes (generally $<10^{-12}$ s^{-1} [*Neuzil*, 1995]) is such that they may be important in creating overpressures when moderately large regions of a flow domain ($L > 100$ m) are composed of or bounded by material with $k \leq 10^{-17}$ m^2 (Figure 1).

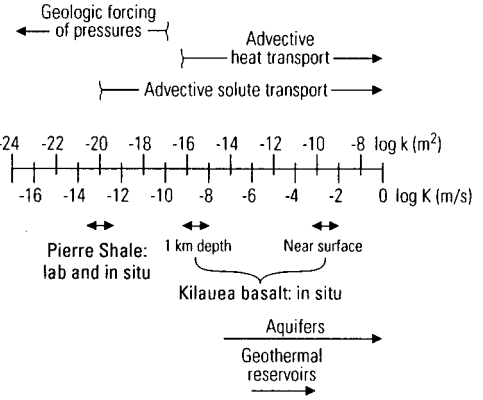

Figure 1. Range of permeabilities observed in geologic media, showing approximate process-limiting values under upper crustal conditions and other selected values discussed in the text. Permeability (k, m^2) and hydraulic conductivity ($K = k\rho_f g/\mu$, m s^{-1}) are related for water density ρ_w and viscosity μ_w at 15°C.

3.2. Heat Transport

The coupling between fluid flow and heat transport was described by *Stallman* [1960], and *Bredehoeft and Papadopulos* [1965] presented a solution to Stallman's general heat transport equations for the particular case of uniform upflow between constant-temperature boundaries:

$$(T_z - T_U)/(T_L - T_U) = f(\beta, z/L) \quad (5)$$

where

$$f(\beta, z/L) = [\exp(\beta z/L) - 1]/[\exp(\beta) - 1],$$

$$\beta = c_w \rho_w q_w L/K_m,$$

T_U, T_L, and T_z are temperatures at the upper and lower boundaries and at an intermediate depth z, L is the distance between the constant-temperature boundaries, c_w is the heat capacity of liquid water, q_w is the volumetric fluid flux or flow rate defined by Darcy's law (q_x of equation (1)), and K_m is the thermal conductivity of the porous medium. The value of z is zero at the upper boundary and increases downward, and the dimensionless number β is negative for upflow and positive for downflow.

Choosing a temperature range of 100°–200°C, a length scale of 400 m, and a typical value of 2 W (m-K)$^{-1}$ for K_m, we have plotted temperature solutions for a series of flow rates in Figure 2a. A flow rate q_w of 10^{-10} m s^{-1} (0.3 cm yr^{-1}) corresponds to an advective heat flux of 40–70 mW m^{-2} and causes a subtle but detectable curvature. Larger flow rates cause pronounced curvature, whereas lower rates result in linear temperature profiles, indicating that heat transport is mainly by conduction. The mean continental conductive heat flux is about 60 mW m^{-2} [*Jessop et al.*, 1976], so if vertical flow rates are as large as 10^{-9} m s^{-1} (3 cm yr^{-1}), advection is likely the dominant mode of vertical heat transport, even if temperatures are substantially lower than those used in our example.

Threshold flow rates for advection of heat (and solutes) over various length scales were clearly elucidated by *Bickle and McKenzie* [1987]. A useful extension of this analysis would be to translate the threshold flow rates for heat advection into permeabilities. This is a somewhat ambitious task because the threshold flow rate depends on the overall temperature difference as well as

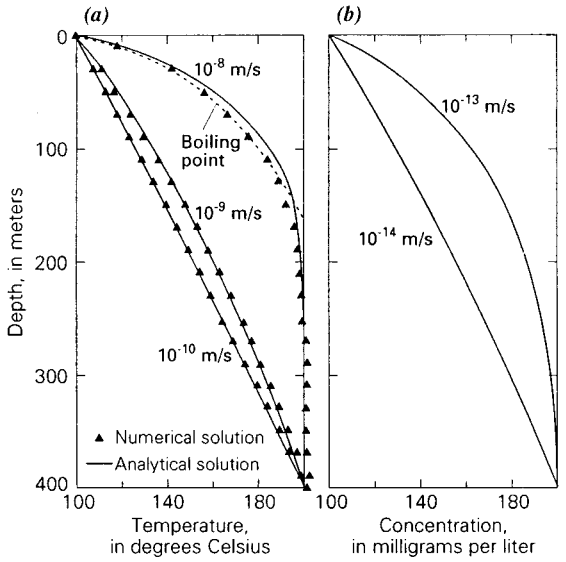

Figure 2. Steady-state solutions for one-dimensional fluid flow with (a) transport of heat and (b) transport of a nonadsorbing solute. Temperatures and concentrations are held fixed at the upper and lower boundaries. Note that the temperature profile remains nearly linear at flow rates that are sufficient to greatly perturb the concentration profile. For the uppermost curve in Figure 2a, triangles indicate solutions for boiling fluid obtained with the HYDROTHERM model [*Hayba and Ingebritsen*, 1994].

the length scale (equation (5)). The flow rate in turn depends on hydraulic gradients (equation (1)) as well as on hydraulic conductivity.

We approached this problem by first assuming a particular hydraulic gradient and then calculating threshold permeabilities for the heat transport problem over length (ΔL = 1 m to 1 km) and temperature (ΔT = 10°–100°C) scales that encompass many problems of geologic interest. (For many "crustal"-scale processes with apparent length scales of ≥10 km, fluid production may actually be occurring in a subset of the domain, for example between metamorphic isograds.) The fixed hydraulic gradient was chosen to be 10 MPa km^{-1}, equivalent to a unit head gradient at standard temperature and pressure. This is a reasonable maximum for flow in upper crustal regions where fluid pressures vary about the hydrostatic gradient. The hydraulic gradient in middle to lower crustal regions where fluid pressures approach lithostatic may be somewhat larger (up to ~20 MPa km^{-1}).

The threshold permeability for "significant" advective heat transport was taken as the value at which advective and conductive heat transport are equal; that is, the value required for a thermal Nusselt (Nu) number of 2, with Nu defined as

$$\frac{[c_w \rho_w q_w T + K_m[(T_L - T_U)/L]]}{K_m[(T_L - T_U)/L]}, \qquad (6)$$

using the same notation as equation (5) and taking $T = (T_L + T_U)/2$. The threshold permeabilities were calculated over pressure-temperature ranges of 0–1,000 MPa and 0°–1000°C using the U.S. Geological Survey model HYDROTHERM [*Hayba and Ingebritsen*, 1994] (http://h2o.usgs.gov/software/hydrotherm.html).

Examination of the results shows a 10^4-fold difference in threshold permeability values between cases with small length scales and large temperature differences (perhaps corresponding to intense contact metamorphism) and cases with large length scales and small temperature differences (perhaps corresponding to high pressure–low temperature metamorphism) (Figure 3). For any particular $\Delta L - \Delta T$ pair there is a 10^2-fold difference in the threshold permeability due to variations in fluid properties (ρ_f, μ_f) across the pressure-temperature range considered.

3.3. Solute Transport

Whereas a linear temperature profile indicates that heat transport is dominantly by conduction, a linear solute concentration profile indicates that solute transport is dominantly by molecular diffusion. In each case, departures from linearity imply that advection may be significant. Written in the same form as equation (5) and assuming that $C_L > C_U$, the solution for the solute transport problem of steady flow between constant-concentration boundaries is [e.g., *Bickle and McKenzie*, 1987; *Finlayson*, 1992]

$$(C_z - C_U)/(C_L - C_U) = f(\xi, z/L) \qquad (7)$$

where

$$f(\xi, z/L) = [\exp(\xi z/L) - 1]/[\exp(\xi) - 1];$$

$$\xi = q_w L/nD;$$

C_U, C_L, and C_z are concentrations at the upper and lower boundaries and at an intermediate depth z; L is the distance between the constant-concentration boundaries; D is a dispersion-diffusion coefficient; n is porosity; and the dimensionless parameter ξ is negative for upflow and positive for downflow. Whereas thermal conductivity can often be treated as a simple constant (K_m in (5) and (6)), the dispersion-diffusion coefficient D is a velocity-dependent parameter that can be expressed as

$$\alpha_L q_w/n + D_m, \qquad (8)$$

where α_L is known as the longitudinal dispersivity and, in porous-media applications, D_m is some fraction of the coefficient of molecular diffusion in Fick's first law. For common, nonadsorbed dissolved species, values of D_m are generally in the range of 10^{-11}–10^{-9} m^2 s^{-1} [e.g., *Freeze and Cherry*, 1979]. The dispersivity α_L is generally regarded as a scale-dependent parameter, and for flow path lengths of the order of 10^2 m, values for α_L of 1–10 m are considered reasonable [e.g., *Gelhar et al.*, 1992].

For typical values of α_L (5 m), D_m (10^{-10} m^2 s^{-1}), and n (0.1), the effects of advection on the concentration profile become obvious at flow rates that are about 10^4

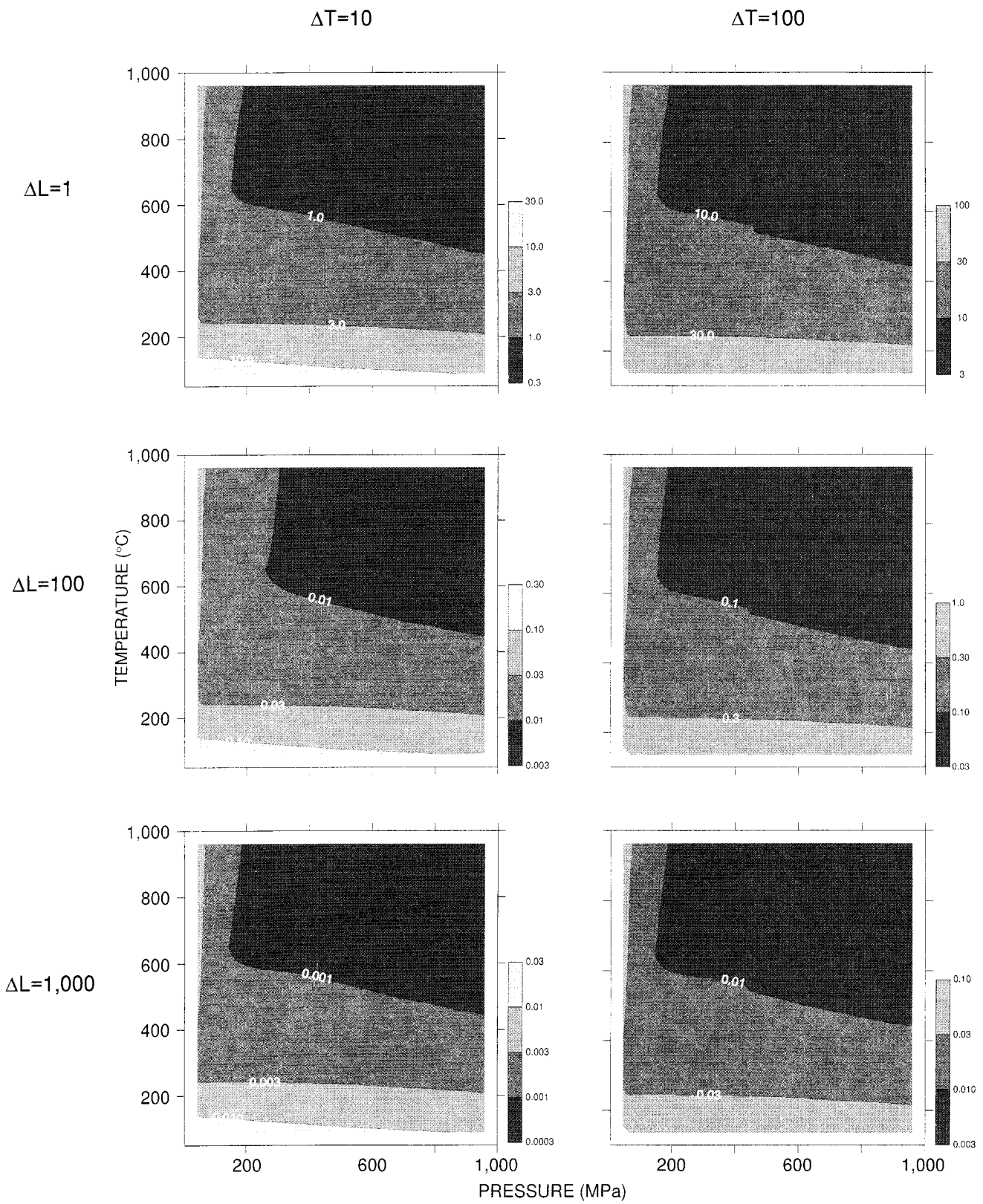

Figure 3. Permeabilities required for a thermal Nusselt number of 2 for selected values of ΔL and ΔT, a hydraulic gradient of 10 MPa km^{-1}, and a medium thermal conductivity of 2 W $(m\text{-}K)^{-1}$. Units of permeability are $m^2 \times 10^{-16}$.

times smaller than those required to perturb the temperature profile (Figure 2b). At these rather low flow rates (10^{-14}–10^{-13} m s^{-1}) the dispersive solute flux is negligible ($\alpha q_w/n < 5 \times 10^{-12}$ m^2 s^{-1}), and the curvature of the concentration profiles is controlled only by the competing influence of advection ($v_w C$) and molecular diffusion ($D_m = 10^{-10}$ m^2 s^{-1}). As *Bickle and McKenzie* [1987] realized, the large difference between the threshold flow rates for advective transport of heat and solutes simply reflects the relative efficiency of conduction as a heat transport mechanism as compared with molecular diffusion as a solute transport mechanism.

Bickle and McKenzie [1987, p. 389] subdivided fluid flow regimes into three classes as a function of flow rate and transport distance: "... one in which advection of both heat and matter [solute] predominate, a second in which heat is largely conducted but matter is advected, and a third in which advection of both heat and matter is insignificant." As we shall show in the next section, geothermal data indicate that upper crustal (≤10 km) hydrologic systems span the boundary between the first and second classes. Later, we summarize data from metamorphic systems deeper in the crust; these data indicate that regions of active metamorphism typically fall in the second class (heat advection insignificant but advection of matter significant).

4. CRUSTAL PERMEABILITY: INFERENCES FROM GEOTHERMAL DATA

In this section we summarize results obtained by using geothermal data from a variety of settings to estimate homogeneous, isotropic crustal permeabilities on a large scale, a scale beyond that measurable by in situ hydraulic testing. A number of workers have used geothermal data to constrain the permeabilities of sedimentary basins and other geologic environments. Consideration of these studies as a whole (Table 1, appendix) suggests some general conclusions about crustal permeability within the depth range explored by geothermal studies (usually <3 km but sometimes as deep as 10 km).

4.1. A Hypothetical Example

For regional groundwater flow under quasi-rectangular geometries and uniform water table slopes, *Domenico and Palciauskas* [1973] showed that significant advective perturbation of the thermal field can be expected when the dimensionless ratio

$$\frac{\rho_w^2 c_w k g B \Delta z}{2 \mu_w K_m L}, \qquad (9)$$

reaches a value of the order of 1, where B is basin thickness, Δz is the water table relief, and L is basin length. (Note the analogy between this ratio and the β ratio of (6). Here, $\rho g k \Delta z/\mu_w L$ approximates a basin-scale flow rate and is thus analogous to q_w in (6). Both β and the dimensionless ratio here are thermal Peclet numbers.) This simple analytical approach for homogeneous, isotropic systems can be compared with numerical simulation results, which also serve to illustrate basic aspects of basin-scale heat transfer (Figure 4). *Smith and Chapman* [1983] simulated a 5-km-deep by 40-km-long basin with a linearly sloping water table and 500 m of total water table relief, a relatively large vertical/horizontal aspect ratio and large water table slope that might apply, for example, to some of the intermontane basins of the western United States. They considered a range of permeabilities over which heat advection was negligible (1×10^{-18} m^2) to highly significant ($>10^{-16}$ m^2). At a permeability of 5×10^{-16} m^2, for example, heat flow varies from 20 mW m^{-2} at the recharge margin of the basin to 160 mW m^{-2} at the discharge margin, and temperatures at similar depths in the recharge and discharge areas differ by as much as 50°C. By evaluating fluid properties (ρ_w, μ_w, c_w) at the average basin temperature of about 90°C, we can use (9) to translate the permeabilities of Figure 4 to modified Peclet numbers of 0.002, 0.3, and 0.8. The threshold permeability for significant advective perturbation is in fact of the order of 1.

4.2. Some General Conclusions Based on Heat-Flow Observations

Analyses of coupled groundwater flow and heat transport in the upper crust typically infer permeabilities in the range of 10^{-17}–10^{-14} m^2, with a distribution that is positively skewed about a mean value somewhat greater than 10^{-16} m^2 (Table 1). This mean value is lower than the average crustal permeability suggested by *Brace* [1984] by about 2 orders of magnitude. However, Brace was working mainly with shallow data, generally from <500-m depth. *Clauser*'s [1992] more recent compilation of in situ permeability data from crystalline rocks includes data from several relatively deep holes, and the mean of these data is significantly lower.

Studies concluding that heat transport is conduction dominated typically infer limiting permeability values of $<10^{-17}$ m^2 to $\leq 10^{-15}$ m^2, depending on the geometry and dimensions of the system. Such values are generally consistent with the limiting value for heat advection (10^{-16} m^2) inferred in many analyses of magmatic-hydrothermal systems [*Norton and Knight*, 1977; *Manning et al.*, 1993; *Ingebritsen and Hayba*, 1994; *Hayba and Ingebritsen*, 1997]. In light of the extreme range of threshold permeabilities for heat advection depicted in Figure 3 ($\sim 4 \times 10^{-20}$ to 1×10^{-14} m^2), the consistent report of a particular threshold value of $\sim 10^{-16}$ m^2 based on one- and two-dimensional simulations of hydrothermal systems may seem puzzling. However, simulations with values of ΔL (1 km), ΔT (250°C), and ΔP (1 MPa) believed representative of magmatic-hydrothermal systems (not shown) lead to threshold permeabilities of 0.3–3.0 $\times 10^{-16}$ m^2 in the pertinent pressure-temperature range.

TABLE 1. Permeabilities From Analyses of Groundwater Flow Constrained by Geothermal Data

Locality	*Environment*	*Depth, km*	*log k*, m^2			*Notes*
			Thermal Models	*In Situ*	*Core*	
Uinta basin, Utah	sedimentary basin	0–3	−14.3 to −13.5	−12.3	−13.9	In situ and core values are geometric means.
North Slope, Alaska	sedimentary basin	0.5–7	−13.6 to −12.6 (k_x) −16.0 to −15.3 (k_z)	−15.7 to −12.7	−13.2 (k_x) −15.7 (k_z)	Core values are arithmetic (k_x) and harmonic (k_z) means.
Arkoma basin	sedimentary basin	0–5	≤−15			
Rhine graben	sedimentary basin	0.3–5.3	−14.5 to −14.2			
Coast Ranges, California	active mountain belt	0–1	−17 to −15			Thermal models apply to various regions; core and in situ data are from Cajon Pass drill hole.
		1–5	≤−16.6			
		5–10	≤−17.5			
		10–15	≤−18.5			
		1.8–1.9		−18.3		
		1.8–2.1		−17.8		
		0.3–2.1			−21.0 to −16.3	
Cascade Range	volcanic rocks	<∼1.5	≥−14			Rocks from <∼1.5 km are ≤2 Ma; those from ≥∼4 km are ≥18 Ma.
		1.5–4	−14 to −16			
		>∼4	≤−16			
Hawaii	volcanic rocks	0.5–1.2	−13.2	−14		
		>1	<−15	−16		
Jura Overthrust	crystalline basement	3–7	−15.5 to −14.5			
Kola well	crystalline basement	0–2	−14.3 to −14.1			Thermal models constrain k only to 8 km because downhole T data are inaccurate below that depth; core value is geometric mean at 1 kbar ±1σ.
		2–4	−15.0			
		4–6	−16.0			
		6–8	−17.0			
		3.8–9.9			−16.3 ± 0.7	
KTB wells	crystalline basement	1–9.1	≤−17			In situ range ignores low-quality injection data; core value is pressure-corrected geometric mean ±1σ.
		0.3–9.1		−17.2 to −15.4		
		0–7.4			−19.1 ± 1.2	

Volcanic rocks from Hawaii are included to represent permeabilities that might occur in continental volcanic provinces such as the Columbia Plateas or rift zones. Permeability values are listed as maxima where heat flow was found to be conductive; k in such cases cannot exceed the given value without introducing a significant advective component to the heat flow. Data sources are as follows: Uinta basin, *Willet and Chapman* [1989]; North Slope, *Deming* [1993]; Arkoma basin, *Lee et al*. [1996]; Rhine graben, *Clauser* [1989]; Coast Ranges, *Williams and Narasimhan* [1988], *Coyle and Zoback* [1988], and *Morrow and Byerlee* [1989]; Cascades, *Ingebritsen et al*. [1992]; Hawaii, *Murray* [1974] and *Ingebritsen and Scholl* [1993]; Jura, *Griesser and Rybach* [1989]; Kola, *Bayuk et al*. [1987] and *Kukkonen and Clauser* [1994]; KTB, *Clauser et al*. [1997], and *Huenges et al*. [1997].

Recognizing 10^{-16} m^2 as the approximate threshold value for significant advective heat transport in a fairly wide range of upper crustal contexts, the roughly 10^4 disparity between the threshold flow rates for significant advection of heat and solutes (Figure 2) indicates that the threshold permeability for advection of solutes will often be of the order of 10^{-20} m^2 (Figure 1). Higher threshold permeability values for both processes may pertain locally, for instance during contact metamorphism, and lower values may apply to flow regimes deeper in the crust, where both length scales and hydraulic gradients are likely to be large.

Geothermal studies in the Uinta and North Slope basins and in the crystalline continental crust of northern Europe provide some insight into the relation between in situ and regional-scale permeability values (Table 1, appendix). These data do not support an increasing trend in the value of permeability between in situ and "regional" scales but are fairly consistent with *Clauser*'s [1992] compilation of crystalline rock data, which showed good agreement between the overall in situ and regional permeability ranges. Some of the inferred regional-scale permeabilities are lower than the in situ values. In some instances, this could be caused by sample bias, with high-permeability layers oversampled by in situ tests (e.g., in the Uinta basin case [*Willett and Chapman*, 1987]). In other instances, the in situ tests may have sampled permeable fracture networks that are discontinuous on a regional scale.

5. CRUSTAL PERMEABILITY: INFERENCES FROM METAMORPHIC SYSTEMS

In the preceding section we reviewed permeability estimates based on geothermal data and drew general

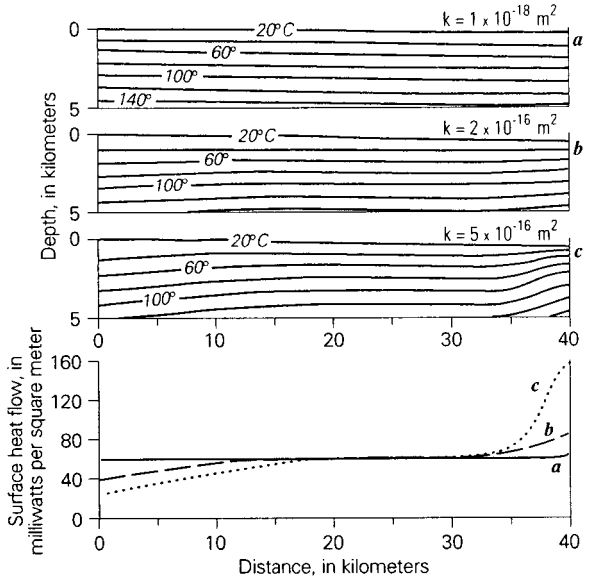

Figure 4. Results from numerical simulation of a 40-km-long by 5-km-deep sedimentary basin, for three different values of homogeneous, isotropic permeability. A total of 500 m of water table relief (a linear slope of 1:80) drives groundwater flow from left to right. Heat flow at the base of the system is 60 mW m^{-2}, and the medium thermal conductivity is approximately 2.5 W $(m\text{-}K)^{-1}$. From *Smith and Chapman* [1983].

conclusions based on the suite of published estimates from various geologic environments. Any attempt to draw general conclusions based on data from metamorphic systems requires a more complete analysis. This is because the primary data from studies of metamorphic systems consist of time-integrated fluid-flux estimates rather than permeability estimates. In some cases, other authors have estimated permeabilities from the time-integrated fluxes, but even in these cases a variety of approaches has been employed. In order to compare results from various studies, we must consider their primary data in a self-consistent fashion.

Evidence accumulated over the last 20 years indicates that fluid migration during metamorphism is common on a range of scales in all crustal settings. The framework for understanding the hydrology of metamorphic systems has been enhanced by numerical modeling of upper crustal hydrothermal and contact-metamorphic systems [e.g., *Norton and Knight*, 1977; *Norton and Taylor*, 1979; *Norton and Cathles*, 1979; *Hanson*, 1992, 1995; *Hayba and Ingebritsen*, 1997] and mid and lower crustal regional metamorphic systems [e.g., *Connolly and Thompson*, 1989; *Connolly*, 1997b; *Hanson*, 1997]. These studies have provided broad constraints on the hydrodynamics of metamorphic fluid flow. At the same time, advances in metamorphic petrology have made it possible to quantify certain hydrologic parameters, including permeability, as recorded by exhumed metamorphic terranes. In this section we review the nature of metamorphic fluid flow and summarize existing constraints on permeability in these systems.

5.1. Evidence for Large Fluid Fluxes in Metamorphic Rocks

In principle, metamorphism need not occur in the presence of a fluid phase [*Thompson*, 1983]. However, it has become increasingly apparent that fluids play a central role in the metamorphism of the Earth's crust [e.g., *Walther*, 1994]. In many cases the sources of metamorphic fluids are local and transport length scales short, but there is growing evidence for fluid migration over hundreds to thousands of meters [e.g., *Oliver*, 1996]. This evidence includes (1) loss of volatile species contained in the protoliths of metamorphic rocks; (2) loss or addition of nonvolatile components in excess of that possible through interaction with locally derived fluids, as recorded by bulk compositional shifts, pressure solution, concentration of ore minerals, and the development of veins containing metamorphic minerals; (3) shifts in light stable isotope compositions that require interaction between metamorphic rocks and an infiltrating fluid; (4) petrologic evidence for flowing fluids driving metamorphic reactions; and (5) the compositions of certain fluids from seeps, springs, and geothermal systems that indicate extensive water-rock reaction at the elevated pressures and temperatures of metamorphism [e.g., *Fyfe et al*., 1978; *Etheridge et al*., 1983, 1984; *Rumble*, 1989, 1994; *Ferry*, 1994a]. These hallmarks of fluid flow over large length scales have been found even at the deepest crustal levels (i.e., from 20 km to the base of the crust) in granulites [e.g., *Newton et al*., 1980; *Harris and Bickle*, 1989; *Harley and Buick*, 1992; *Harris et al*., 1993; *Harley and Santosh*, 1995], vein systems [*Ague*, 1994, 1995], and shear zones [e.g., *Austrheim*, 1987; *Fourcade et al*., 1989; *Jamtveit et al*., 1990; *Newton*, 1990; *Fruh Green*, 1994; *Mattey et al*., 1994; *Austrheim and Engvik*, 1997]. The magnitude of permeability, regardless of crustal environment, must have been sufficient to accommodate the flow recorded by the exhumed metamorphic rocks.

5.2. Metamorphic Hydrology

5.2.1. Controls on the pore network. The variation in rock strength with depth dictates that the evolution of permeability and fluid flow should be different in the strong, brittle upper crust relative to the weak middle and lower crust [e.g., *Connolly and Thompson*, 1989]. The high strength of the crust in the brittle regime (to depths of 10–15 km) allows connected pore networks to occur over a wide depth range. This allows near-hydrostatic fluid pressure gradients over large length scales and geologically significant times. In addition, small departures from the hydrostatic gradient (typically <1 MPa km^{-1}) due to topography and/or thermal perturbations can drive significant fluid migration. Under near-hydrostatic conditions, surface (meteoric) fluid can circulate to significant depths. Because of their distinct isotopic composition at appropriate latitudes and elevations, surface fluids act as a tracer for fluid migration and

were historically important in the recognition of fluid migration in metamorphic environments [e.g., *Taylor and Forester*, 1979; *Taylor*, 1990]. In crystalline rocks, near-hydrostatic fluid pressures can persist to depths of at least 9–10 km [e.g., *Huenges et al*., 1997; *Zoback and Zoback*, 1997].

Below the relatively strong upper crust, rocks weaken significantly owing to deformation mechanisms involving creep, which may occur by crystal plasticity or solution-precipitation mechanisms [e.g., *Cox and Etheridge*, 1989; *Cox and Paterson*, 1991; *Rutter and Brodie*, 1995]. Evidence for a fundamental change in metamorphic hydrology at a depth broadly consistent with the brittle-plastic transition is found in the form of hydraulic fractures produced by devolatilization reactions, which are related to a drop in fluid pressure from lithostatic to near-hydrostatic values [*Coombs*, 1993]. Permeability may decrease with depth beyond this interval as a result of progressive changes in pore distribution, shape, and connectivity [*Fischer and Paterson*, 1992; *Gavrilenko and Geugen*, 1993].

Once metamorphism ensues and a fluid phase is produced by metamorphic devolatilization reactions or introduced from an external source, fluid pressure can quickly rise to near-lithostatic values. Hydraulic fracturing will occur when the fluid pressure exceeds the sum of the least principal stress and any tensile strength of the rock mass [e.g., *Hubbert and Willis*, 1957; *Bredehoeft et al*., 1976; *Raleigh et al*., 1976; *Etheridge*, 1983]. Whereas empirical observations in the upper crust indicate that this can occur at fluid pressures as low as ~1.25 times hydrostatic, phase equilibria and fluid inclusions in metamorphic rocks from deeper crustal settings typically indicate that fluid pressure is close to the lithostatic load [e.g., *Fyfe et al*., 1978]. Uncertainties in metamorphic fluid pressures are usually large, but in a unique study, *Holdaway and Goodge* [1990] showed that slightly sub-lithostatic fluid pressures occurred in mica schists (P_f = 0.95 lithostatic), whereas adjacent quartzites record lithostatic fluid pressures.

In general, fluid pressures appear to be maintained at or near lithostatic during metamorphism, consistent with the expectation that rocks will fail near this value. Fluid pressures elevated well above the local hydrostat imply that the time- and volume-averaged path of fluid flow will be toward the Earth's surface. Such flow is inherently episodic [e.g., *Walder and Nur*, 1984; *Gold and Soter*, 1985; *Nur and Walder*, 1990] and is coupled with rock deformation through the balance between crack formation and sealing processes [e.g., *Etheridge et al*., 1984; *Oliver*, 1996]. If permeability remains low, fluids are transported by propagating hydraulic fractures [e.g., *Emmerman et al*., 1986; *Nishiyama*, 1989; *Nakashima*, 1993, 1995]. Higher permeabilities can be created by compaction-related dilatency due to dehydration, which leads to upward propagating porosity waves nucleated at the fluid source and leaving a connected pore network in their wake [*Connolly*, 1997b].

It is important to recognize that although the fluid pressure regime dictates dominantly vertical fluid flow, significant local departures from vertical flow may arise from permeability heterogeneities. In fact, one of the major issues in crustal petrology today is reconciling the results of numerical models [e.g., *Hanson*, 1997], which predict subvertical (upward), downtemperature flow, with field-based studies that infer subhorizontal, uptemperature flow [e.g., *Ferry*, 1992; *Skelton et al*., 1995]. The simplest explanation is that local heterogeneities due to lithology, metamorphic foliation, or folding [*Skelton*, 1996] temporarily deflect flow path lines from their dominantly vertical orientation.

5.2.2. Applicability of Darcy's law. In the absence of a fluid phase, permeability and porosity in the middle and lower crust are exceedingly small. Under these conditions, permeability is controlled by grain boundary geometry [e.g., *Watson and Brenan*, 1987; *Holness*, 1992, 1993, 1997], fluid migration is driven by surface tension or diffusion in an adsorbed grain boundary film of fluid [e.g., *Walther and Orville*, 1982; *Brenan*, 1991], and flow is not Darcian [e.g., *Swartzendruber*, 1962]. However, a wealth of evidence indicates that this scenario is unlikely during metamorphism (see reviews by *Ferry* [1994a] and *Rumble* [1994]). Deformation during metamorphism leads to creation of a connected pore network. While the length and time scales of this pore network are highly variable and the controls on its development remain poorly understood, it is clear that permeability can be maintained for geologically significant times [*Ferry*, 1994a; *Oliver*, 1996]. Large-scale migration of a fluid phase that pervades the rock matrix on scales approaching those of the grain size is termed "pervasive flow" or "infiltration" by metamorphic petrologists and is favored by low strain rates and homogeneous lithologies and permeability [*Oliver*, 1996]. Systems with higher strains and a more heterogeneous rheology and permeability favor focusing of fluid into narrow regions, which may be individual lithologic units, portions of units, or fractures. This condition is referred to as "channeled" flow.

Regardless of whether flow is channeled or pervasive, Darcy's law can be used to assess the links between fluid flux and the driving-force gradient, because the rocks behave as a porous medium or its equivalent when averaged over time and volume. However, in some environments the spatial-averaging scale required for realistic application of Darcy's law may be impractically large; for instance, crustal faults and the giant hydrothermal veins found in some ore deposits may channel large volumes of fluid and influence regional flow patterns. Here we will focus on systems and scales of observation for which a porous-medium-equivalent approach seems reasonable, excluding major fault zones and giant veins.

5.3. Metamorphic Permeability

5.3.1. Approaches to estimation. Metamorphic systems are far removed from the Earth's surface, where direct observation is possible. As was discussed in the introduction, extrapolation of average permeability values derived from near-surface measurements, with or without an assumed depth dependence, is fraught with problems. In general, there are three possible approaches to determining metamorphic permeability more rigorously: (1) direct determination through characterization of the pore network as preserved in exhumed metamorphic rocks, (2) simulations constraining feasible permeability ranges, and (3) inference from the fluid fluxes recorded by rock chemistry or reaction history.

Direct determination of permeability is impossible in metamorphic rocks because the pore network is modified by the integrated effects of chemical reactions and deformation during and after fluid flow. In principle, if porosity during metamorphism can be estimated or measured, porosity-permeability relations can be used to estimate permeability. Computed X-ray microtomography or quantitative image analysis holds great promise for reconstructing pore networks and simulating flow [e.g., *Ehrlich et al*., 1991; *Spanne et al*., 1994; *Auzerais et al*., 1996; *Blair et al*., 1996; *Mowers and Budd*, 1996; *Sardini et al*., 1997], but these techniques have not yet been applied to metamorphic rocks. Similarly, vein abundance can be measured and vein porosity can be related to permeability [e.g., *Snow*, 1970]. In general, however, such studies must assume that the currently preserved pore network is an accurate representation of the average properties of the system of interest, when in fact it represents the cumulative porosity integrated over the duration of fluid flow and fails to record possible poroelastic contributions [e.g., *Manning and Bird*, 1991]. While measured vein porosities may produce reasonable permeabilities in some cases [e.g., *Norton et al*., 1984], they may lead to serious errors in permeability in others.

A second technique for estimating permeability involves analytical or numerical studies of coupled fluid flow and heat or solute transport [e.g., *Norton and Knight*, 1977; *Norton and Cathles*, 1979; *Bickle and McKenzie*, 1987; *Connolly and Thompson*, 1989; *Connolly*, 1997a; *Hanson*, 1992, 1995, 1997]. This approach is extremely useful for establishing permissible ranges in permeability. However, it can only constrain the average permeability for specific systems when combined with other methods, such as thermometry and mass transfer calculations.

Finally, permeabilities can be estimated from the time-integrated fluid flux Q recorded by changes in mineral assemblages or rock composition. The time-integrated flux has units of $L^3\ L^{-2}$, mol L^{-2}, or mass L^{-2}, where L is length, and can be determined from analytical solutions to appropriate statements of transport equations [e.g., *Bickle and McKenzie*, 1987; *Baumgartner and Rumble*, 1988; *Bickle and Baker*, 1990; *Baumgartner and Ferry*, 1991; *Dipple and Ferry*, 1992]. When combined with estimates of the duration of the flow event, fluid viscosity, and the driving-force gradient, the time-integrated flux can be used to constrain time-averaged permeability. This method, alone or in combination with numerical simulations, affords the best estimate of metamorphic permeability. Below, we discuss uncertainties in Q and calculated permeability, and then review fluxes and permeabilities for various metamorphic environments.

5.3.2. Time-integrated fluid flux. Statements of mass conservation allow calculation of the time-integrated fluid fluxes by using the change in fluid composition required by mineral assemblages or stable isotope compositions along an assumed flow path [*Baumgartner and Ferry*, 1991; *Dipple and Ferry*, 1992]. Transport of a component downstream along a pressure-temperature gradient requires adjustment in both fluid composition and mineral modal abundance. This leads to a one-dimensional analytical solution for molar flux of component i [*Baumgartner and Ferry*, 1991]:

$$Q_i = \frac{M_i[1 - X_i\Sigma(\nu_j/\nu_i)]}{dX_i/dx}, \tag{10}$$

where M_i is the number of moles of component i produced or consumed as a consequence of fluid-driven metamorphic reactions, X_i is the mole fraction of i in the fluid phase, x is the distance along the flow path, and ν is the stoichiometric coefficient of the jth species for the equilibrium of interest. The fluid is assumed to be in local equilibrium with its host rock everywhere along the flow path, which requires that the only factor driving reactions is the gradient in fluid composition. Equation (10) states that the molar time-integrated flux (mol L^{-2}) is equal to the change in the number of moles of species i in the fluid phase due to reaction divided by the change in fluid composition with distance along the flow path. Similar equations based on gradients in stable isotopic ratios allow independent calculations of time-integrated fluid flux [*Dipple and Ferry*, 1992].

The accuracy of time-integrated fluxes derived from (10) or analogues depends strongly on pressure and temperature along the presumed flow path. This is because estimating the pressure or temperature of metamorphic mineral growth requires accurate and precise knowledge of thermodynamic properties of minerals, mineral solid solutions, and aqueous species, as well as equations of state for typically complex crustal fluids. The combined uncertainties in all thermodynamic data usually translate to a maximum precision in pressure of ±100 MPa and in temperature ±25°C [e.g., *Ferry*, 1992, 1994a]. Another source of uncertainty in flux calculations is the protolith composition. In petrological studies, the fluid flux is proportional to the change in the modal abundances of reacting phases (the ν terms in (10)). The appropriate initial modal mineralogy, which is

destroyed by metamorphism, requires calculation from bulk rock composition through the assumption of isochemical metamorphism, or insolubility of a particular component. These sources of uncertainty can be characterized and accounted for to a reasonable degree.

Two additional issues are potentially much more problematic. First, since (10) is one dimensional, the path of the fluid must be known a priori. In practice, this is accomplished by making assumptions about the geometry of the system of interest, coupled with sensitivity tests in which the relevant equation is applied under different scenarios, so that the most likely can be determined. Although the validity of the final result is difficult to test without performing two- or three-dimensional analysis, judicious choice of the coordinate system usually allows quantitative insights into at least the principal component of the time-integrated flux vector. Second, time-integrated flux estimates are based on the progress of chemical interaction between the rock and the fluid; if a volume of fluid migrates through the rock without chemical interaction, its passage will not be recorded, and the flux will be underestimated. However, because studies of fluid-rock interaction focus on grain-scale processes, and because true fluxes are likely extremely low (millimeters to centimeters per year), the values of time-integrated flux measured from metamorphic rocks probably do not lead to severe underestimates except in cases where fluids are strongly channeled into fault zones or fracture systems.

Figure 5 and Table 2 summarize petrologically or isotopically based fluxes that have been computed for diverse metamorphic environments, lithologies, and grades, including (1) contact metamorphism associated with local heat transport from cooling igneous bodies, which occurs along very high geothermal gradients at shallow crustal levels, typically in rift zones and volcanic arcs; (2) combined contact and regional metamorphism at 5- to 15-km depth, which is typically a consequence of elevated orogen-scale geothermal gradients due to heat transported by magmas in continental volcanic arcs; and (3) regional metamorphism involving mineral-fluid reactions along moderate geothermal gradients at deep (>15 km) crustal levels. Molar time-integrated fluxes have been converted to volumetric equivalents with units of $L^3\,L^{-2}$, or L. Maximum fluxes in contact environments are $\sim 5.3 \times 10^3$ m. Higher values are recorded in regional environments (average, $\sim 5.3 \times 10^3$; maximum, $\sim 6.3 \times 10^4$ m). The distribution of time-integrated fluxes is broadly similar between the different environments, with each distribution skewed toward high fluxes.

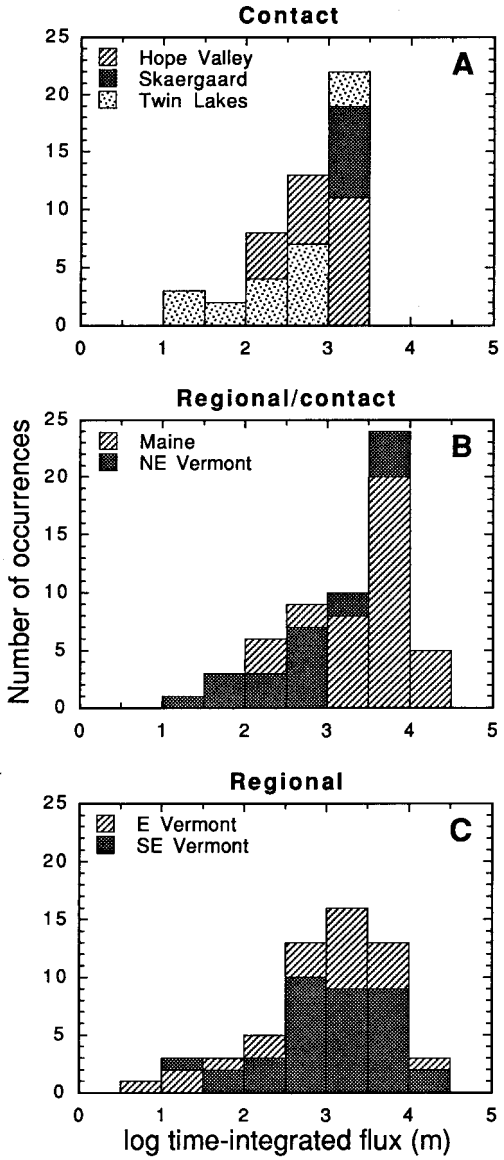

Figure 5. Histograms of time-integrated flux estimates in three types of metamorphic environment where fluxes were computed for individual specimens. Data are from *Ferry* [1989] (Hope Valley), *Ferry* [1992] (SE Vermont), *Davis and Ferry* [1993] (Twin Lakes), *Leger and Ferry* [1993] (NE Vermont), *Ferry* [1994b] (Maine and eastern Vermont), and *Manning and Bird* [1995] (Skaergaard).

5.3.3. Conversion of time-integrated fluxes to permeabilities. Because metamorphic rocks reflect the cumulative effects of mineral-fluid reactions throughout a particular event, the hydrologic parameters that may be derived from them are necessarily integrated with respect to time. Knowledge of the duration of the event (Δt) permits estimation of the time-averaged flux q simply by dividing Q by Δt. While the resulting flux is only an average, and clearly inadequate to understand the changes in the system as metamorphism evolves, these petrologically or isotopically constrained fluxes provide quantitative insights into the magnitudes of fluid flow in different environments. Moreover, they provide a basis for estimating time-averaged permeabilities throughout the continental crust.

Solution of the one-dimensional form of Darcy's law (equation (1)) for time-averaged permeability,

$$k = \left[\frac{Q\mu}{\Delta t[\partial(P + \rho g z)/\partial x]}\right], \qquad (11)$$

TABLE 2. Hydrologic Parameters and Time-Averaged Permeability in Metamorphic Systems

Locality	*Environment*	*Depth, km*	*Lithology*	*log_{10} Q, m*	*Method*	*Driving-Force Gradient, MPa km^{-1}*	*Time, Ma*	*log_{10} k, m^2*
Utah	contact	6.0	carbonate	~3.50	O isotope and numerical model	···	···	−15.6
Greenland	contact	6.0 (2.0)	basalt	3.21 (34)	O isotope and numerical model	···	···	−16.0 (0.5)
Hope Valley, California	contact	7.3 (1.8)	carbonate	3.01 (43)	petrologic	$1^{+6}_{-0.6}$	$0.1^{+0.4}_{-0.05}$	−16.6 (1.2)
Twin Lakes, California	contact	10.9 (1.8)	carbonate	2.37 (49)	petrologic	$1^{+6}_{-0.6}$	$0.1^{+0.4}_{-0.05}$	−17.2 (1.2)
Quebec	contact	14.6 (1.8)	carbonate	2.04 (34)	petrologic	10 (9)	$0.1^{+0.4}_{-0.05}$	−18.2 (1.2)
Maine	regional-contact	12.8 (1.1)	carbonate	3.51 (29)	petrologic	$1^{+6}_{-0.6}$	21^{+11}_{-5}	−18.3 (0.7)
NE Vermont	regional-contact	16.4 (3.6)	carbonate	2.69 (62)	petrologic	$1^{+6}_{-0.6}$	10^{+5}_{-3}	−18.8 (1.0)
Scotland	regional	13.8 (1.8)	pelite	4.48 (34)	Na transport	14 (4)	3^{+4}_{-1}	−17.6 (0.8)
Australia	regional	16.4 (1.8)	pelite	4.96 (34)	O isotope	10 (9)	33^{+34}_{-16}	−18.1 (1.3)
Connecticut	regional	23.7 (5.5)	pelite	4.78 (34)	Si transport	14 (4)	13^{+7}_{-3}	−18.0 (0.5)
SE Vermont	regional	25.5 (3.6)	pelite, sandstone, carbonate	2.80 (61)	petrologic	$1^{+6}_{-0.6}$	10^{+5}_{-3}	−18.7 (1.0)
E Vermont	regional	28.4 (3.6)	carbonate	3.02 (39)	petrologic	$1^{+6}_{-0.6}$	20^{+10}_{-5}	−18.8 (0.8)

Values of Q and k are geometric means. Parenthetical values are uncertainties in last digits for symmetrically distributed errors. Sources of uncertainties are as follows: depth, from authors; Q, combination of standard error in mean and P-T uncertainties; driving-force gradient, from geometrical constraints on flow path assuming $P_f = P_{lithostatic}$; time, from uncertainties in heating rates based on garnet growth [*Christensen et al*., 1989, 1994; *Burton and O'Nions*, 1991; *Vance and O'Nions*, 1992] or numerical models; k, propagated from uncertainties in all parameters. Where uncertainties were not discussed by authors, they were estimated on the basis of average values calculated from *Ferry* [1992, 1994b] and *Léger and Ferry* [1993]. Data sources are as follows: Utah, *Cook et al*. [1997]; Greenland, *Manning et al*. [1993] and *Manning and Bird* [1995]; Hope Valley, California, *Ferry* [1989]; Twin Lakes, California, *Davis and Ferry* [1993]; Quebec, *Cartwright and Weaver* [1993]; Maine, *Ferry* [1994b]; NE Vermont, *Léger and Ferry* [1993]; Scotland, *Ague* [1997]; Australia, *Cartwright et al*. [1995]; Connecticut, *Ague* [1994]; SE Vermont, *Ferry* [1992]; eastern Vermont, *Ferry* [1994b].

illustrates that in addition to the time-integrated flux, the fluid viscosity, driving-force gradient along the flow path [$\partial(P + \rho gz)/\partial x$], and duration of fluid flow must be known. In a few cases authors have used equation (11) to estimate k for metamorphic rocks from time-integrated fluxes. However, their estimates of parameter values and uncertainties have employed a variety of approaches, preventing direct comparison of published k estimates. We will proceed to discuss estimates of the various parameters and their uncertainties in order to develop a self-consistent set of permeability estimates for metamorphic rocks.

Fluids involved in crustal metamorphism are dominated by two molecular components, H_2O and CO_2, which together typically constitute >99 mol% of the fluid phase. Viscosities for the end-members H_2O and CO_2 [*Dudziak and Frank*, 1966; *Walther and Orville*, 1982; *Hayba and Ingebritsen*, 1994] are very similar at crustal metamorphic conditions and only weak functions of pressure and temperature except at very low pressures. Thus although the viscosities of H_2O-CO_2 mixtures are not well characterized, assuming that they are equivalent to pure H_2O is unlikely to introduce significant uncertainty in this parameter.

The driving-force gradient is likely controlled, at least in part, by the brittle-plastic transition and the geometry of the flow path. Numerical simulations of shallow pluton environments in which permeabilities are sufficiently high to maintain near-hydrostatic pressure gradients result in flow in response to thermal buoyancy. The resulting flow at high angles to isotherms arises from the difference in density between hot and cold fluid [*Hanson*, 1995], leading to driving-force gradients of ~1.5 MPa km^{-1} [e.g., *Norton and Taylor*, 1979]. Driving-force gradients are probably substantially larger in most metamorphic environments below 10-km depth. In the deep crust the maximum fluid pressures possible are approximately lithostatic, and under lithostatic conditions the driving force for (upward) fluid flow is the difference between the hydrostatic pressure gradient and the lithostatic pressure gradient $[\rho_{rock} - \rho_{fluid}]g$, for which typical crustal values are 15–20 MPa km^{-1}, depending on the actual distribution of rock and fluid densities. However, it is unlikely that such high vertical fluid pressure gradients are sustained throughout the duration of metamorphic flow events. Experimental [e.g., *Ko et al*., 1997; *Wong et al*., 1997] and theoretical [e.g., *Walder and Nur*, 1984; *Hanson*, 1992, 1995] studies of rock dehydration illustrate that initial buildup of fluid pressures is dissipated by rock failure, such that the resulting metamorphic fluid flow will occur as a consequence of a fluid pressure gradient intermediate between lithostatic and hydrostatic. Using coupled deformation and fluid flow models, *Connolly* [1997b] showed that metamorphic

devolatilization reactions generate porosity waves that propagate through the crust from the site of fluid liberation. Fluid is drained from the source through an interconnected pore network in the wake of this wave. Driving-force gradients are $\sim 14 \pm 4$ MPa km^{-1} for geologically reasonable parameter choices, i.e., between 0.6 and 1 times the value defined by a lithostatic fluid-pressure gradient for typical crustal densities.

Lower values are possible where fluids have a significant horizontal flow component. Subhorizontal fluid flow has been inferred at >10 km depth in regional or contact systems [*Ferry*, 1992, 1994b; *Davis and Ferry*, 1993; *Leger and Ferry*, 1993]. That fluid flow paths had low inclinations from the horizontal (less than ~20°) is in each case required by the observed development of mineral assemblages when compared with the inferred horizontal and vertical variations in pressure and temperature. It is important to note that both the driving-force gradient and the time-integrated fluid flux calculated from observed reaction progress vary with the assumed inclination of the flow path [*Ferry*, 1994a]. For example, varying flow path inclination in the Waterville Formation of south central Maine [*Ferry*, 1994a] from 1° to 15° results in driving-force gradients ranging from 0.6 to 7 MPa km^{-1} for $P_f = P_{total}$. However, the effect on inferred permeability is minor because the calculated time-integrated flux also increases with the flow path angle. This compensating relationship means that estimates of permeability derived from Q do not depend strongly on the driving-force gradient where the geometry of the flow path can be inferred.

Perhaps the greatest uncertainty in the calculation of permeability from time-integrated fluid flux is the duration of fluid flow. Our approach to this problem was to combine heating rates or times derived from isotopic or numerical studies with estimates of the temperature interval of fluid flow. Regional and contact-regional metamorphism in New England localities (Table 2) was associated with Devonian Acadian metamorphism. Garnet growth during this event indicates heating rates of 7.5 ± 2.5 K Myr^{-1} [*Christensen et al*., 1989], which were combined with the inferred metamorphic temperature intervals to estimate the duration of fluid flow. No heating-rate estimates were available for the Australian and Scottish regional metamorphic localities (Table 2). We used average garnet-based heating rates for similar terranes worldwide, which yielded $7.6^{+15}_{-3.8}$ K Myr^{-1} [*Christensen et al*., 1989; *Burton and O'Nions*, 1991; *Vance and O'Nions*, 1992]. Numerical thermal and hydrodynamic models indicate that in contact metamorphic environments the duration of heating and prograde metamorphism, and therefore prograde fluid flow, is $0.5–5 \times 10^5$ years [*Bowers et al*., 1990; *Hanson*, 1995]. These rates and times reflect the overall duration of metamorphism; in some instances, fluid flow may have been active for shorter times, 10^3–10^4 years, on the scale of individual hand samples [*Young and Rumble*, 1993; *Skelton*, 1996; *van Haren et al*., 1996]. It is important to note, however, that samples at these small scales may not represent the system as a whole because different samples may experience flow at different times.

5.3.4. Metamorphic permeabilities. Table 2 summarizes time-averaged metamorphic permeabilities and key parameters used to calculate them for well-characterized metamorphic flow systems, with uncertainties for all estimates. The data show that from 6-km depth to ~30-km depth the permeability of the crust during metamorphism is between $10^{-15.6}$ and $10^{-18.8}$ m^2. There is no systematic dependence on the method used to determine fluid flux, the duration of metamorphism, or the inferred driving-force gradient. Propagation of average uncertainties in all parameters results in an average uncertainty in permeability of ±1.0 decades.

5.3.5. Variation of metamorphic permeabilities with crustal environment. Permeabilities associated with fluid flow in different metamorphic environments are compared in Figure 6, using selected localities where flux determinations were made on numerous samples. Two very different contact environments are compared in Figure 6a. The Skaergaard magma-hydrothermal system is a basalt-hosted gabbro in which fluids were surface derived, depth of metamorphism was ~5 km, and duration of prograde heating was short (~10^4 years). In contrast, the Sierran roof pendants reflect crustal depths of >6 km, prograde heating durations were likely longer (~10^5 years), and fluid sources are unknown for the specific localities, although they are likely to be locally derived magmatic fluids if they are similar to the Ritter Range roof pendant [*Ferry et al*., 1998]. The fluxes are broadly similar in each environment (Figure 6), but permeabilities are higher for the Skaergaard basalts (~10^{-16} m^2) than in the metacarbonate roof pendants ($10^{-18.5}$–10^{-16} m^2). The difference between the two settings depends largely on the duration of fluid flow in this case (equation (11)) but is sensible, given that higher permeabilities should be expected where large path lengths of surface-derived fluids existed, as is demonstrably the case at Skaergaard [*Norton and Taylor*, 1979].

Permeabilities associated with fluid flow in regional-contact metamorphism in Maine and Vermont are lower than those of contact metamorphic environments (Figure 6b). Most fluid flow in these settings is due to regional effects, though locally elevated heat and fluid flow occurs near plutons [e.g., *Leger and Ferry*, 1993]. In regional-metamorphic terranes, mean permeabilities are slightly lower than in shallower metamorphic settings (Figure 6c).

In all three metamorphic environments, permeabilities are skewed toward higher values. Mean permeability decreases from $10^{-16.8}$ m^2 in contact environments, through $10^{-18.5}$ m^2 in regional-contact environments, to $10^{-18.7}$ m^2 for regional metamorphism. Since these environments reflect progressively greater crustal depths (Table 2), our self-consistent data set indicates a decrease in crustal permeability with depth.

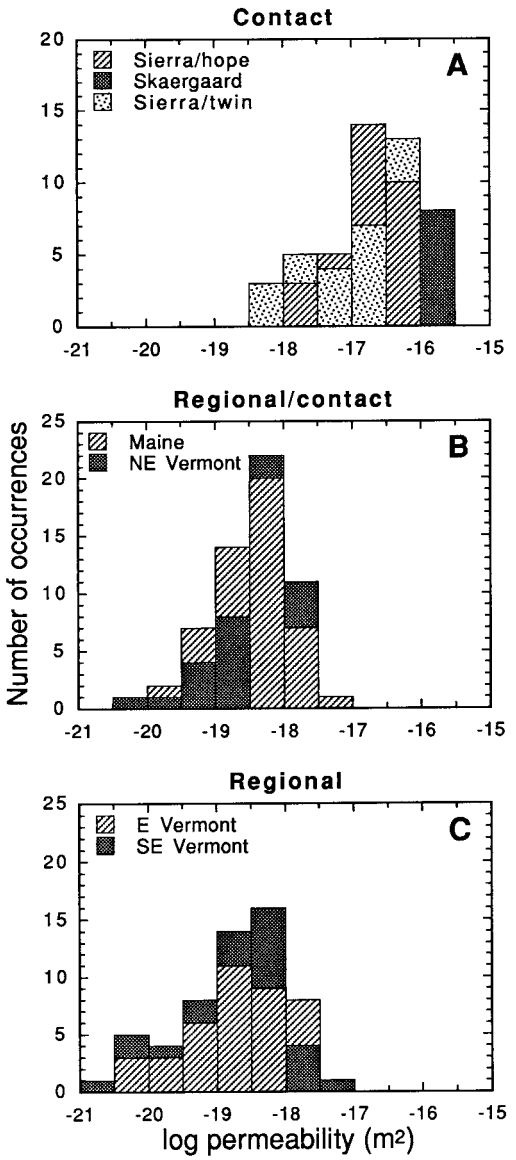

Figure 6. Histograms of metamorphic permeabilities in three types of metamorphic environment. Calculated from the sources listed in the caption for Figure 5.

5.3.6. Lithologic controls. Permeability heterogeneities between different lithologies appear to diminish with depth in the crust. In contact metamorphic environments, basalts and calc-silicate hornfels record the highest permeability, regardless of locality, whereas carbonates record distinctly lower permeability (Figure 7a). Lithological controls are less distinct in the deeper environments of regional-contact and regional metamorphism. In regional-contact environments, pelitic schists have higher average permeabilities than limestones, but there is more overlap of values than in contact environments (Figure 7b). In the deepest settings, all lithologies appear to have similar mean permeability (Figure 7c). Given that all petrologically and isotopically based studies focus on units that experienced fluid flow, heterogeneities on an even greater scale are implicit in this analysis. For example, marbles and quartzites are rarely even studied because they typically record no fluid-rock interaction. This indicates that permeabilities significantly lower than those plotted in Figures 6 and 7 likely exist in any given environment.

6. DISCUSSION AND SUMMARY

The intrinsic permeability of the crust largely determines the occurrence of such geologically significant processes as advective transport via flowing fluids and the generation of elevated fluid pressures. By using simple analyses of homogeneous, one-dimensional systems, thus avoiding full consideration of the issues of

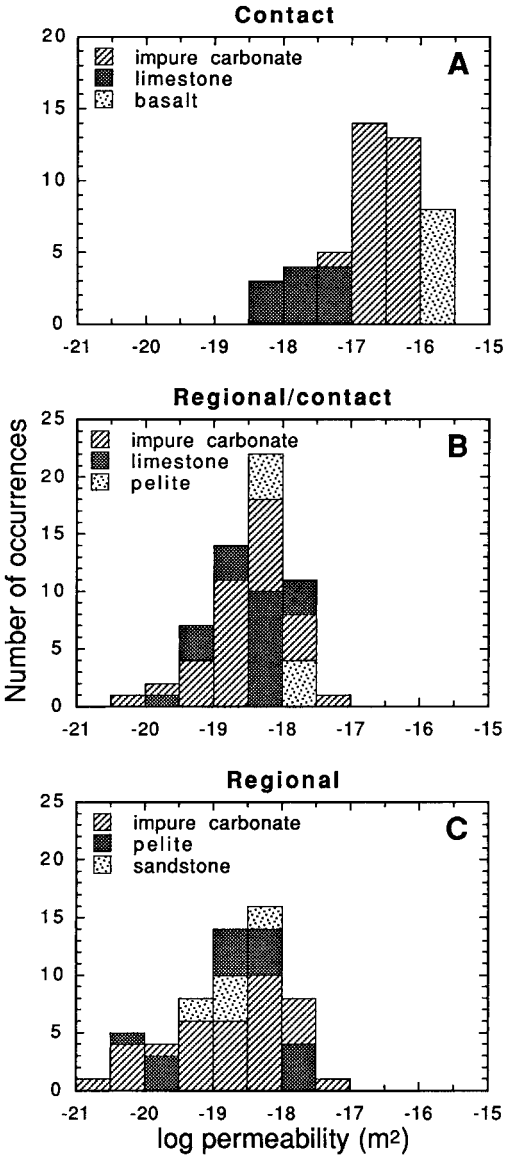

Figure 7. Histograms of metamorphic permeabilities for contact, regional-contact, and regional metamorphic settings, showing differences encountered in different lithologies. Calculated from the sources listed in the caption for Figure 5.

heterogeneity, time, and (apparent) scale dependence of permeability, one can calculate that under upper crustal conditions, significant advective heat transport typically requires permeabilities $k \geq 10^{-16}$ m^2 and advective solute transport $k \geq 10^{-20}$ m^2, whereas elevated fluid pressures generally require $k \leq 10^{-17}$ m^2. The permeability ranges for overpressuring and advective heat transport do not overlap, so that these two processes will generally be mutually exclusive. The highest permeability ranges for advective heat and solute transport do overlap. However, in parts of the upper crust where permeability is in the range of $\sim 10^{-20}$–10^{-16} m^2, heat transport will typically be dominantly by conduction whereas solute transport may be dominantly by advection.

Two classes of independent constraints allow estimation of crustal permeability at large scales and throughout the entire thickness of the continental crust, namely, those afforded by observations of crustal heat flow (Table 1) and studies of metamorphic systems (Table 2). Analyses of coupled groundwater flow and heat transport in the upper crust typically infer permeabilities in the range of 10^{-17} to 10^{-14} m^2, with a distribution that is positively skewed about a mean value somewhat greater than 10^{-16} m^2. This mean value is lower than the average crustal permeability suggested by *Brace* [1984] by about 2 orders of magnitude but is reasonably consistent with *Clauser*'s [1992] more recent compilation of permeability data. The heat-flow-based permeability estimates do not support an increasing trend in the value of permeability between in situ and "regional" scales but, again in accordance with *Clauser*'s [1992] compilation, show generally good agreement between the overall in situ and regional permeability ranges.

Though most heat flow observations pertain to shallow crustal depths, analyses of metamorphic systems permit inferences about permeability deeper in the crust. In regions of active metamorphism it appears that a geochemically significant level of permeability can exist throughout the crust. In active metamorphic systems in the mid to lower crust, the permeabilities required to accommodate the estimated fluid fluxes decrease from $\sim 10^{-16}$ m^2 to $\sim 10^{-18}$ m^2 between 5- and 12-km depth. Below ~12 km, which broadly corresponds to the brittle-plastic transition, k is effectively constant at $\sim 10^{-18.5 \pm 1}$ m^2 (Figure 8a).

Consideration of the permeability values inferred from thermal modeling and metamorphic systems suggests a quasi-exponential decay of permeability with depth (z) of $\log k \approx -3.2 \log z - 14$. To some extent, this is an expected consequence of the generally larger and more heterogeneous permeabilities known to exist in the brittle upper crust. Yet there is an unexpected and pleasing consistency between the deepest in situ and heat-flow-based values and the shallowest metamorphic-system values. The constant in the fit equation, which gives k at 1 km, is similar to *Brace*'s [1984] average crustal value, which is sensible because his compilation strongly weighted near-surface permeability.

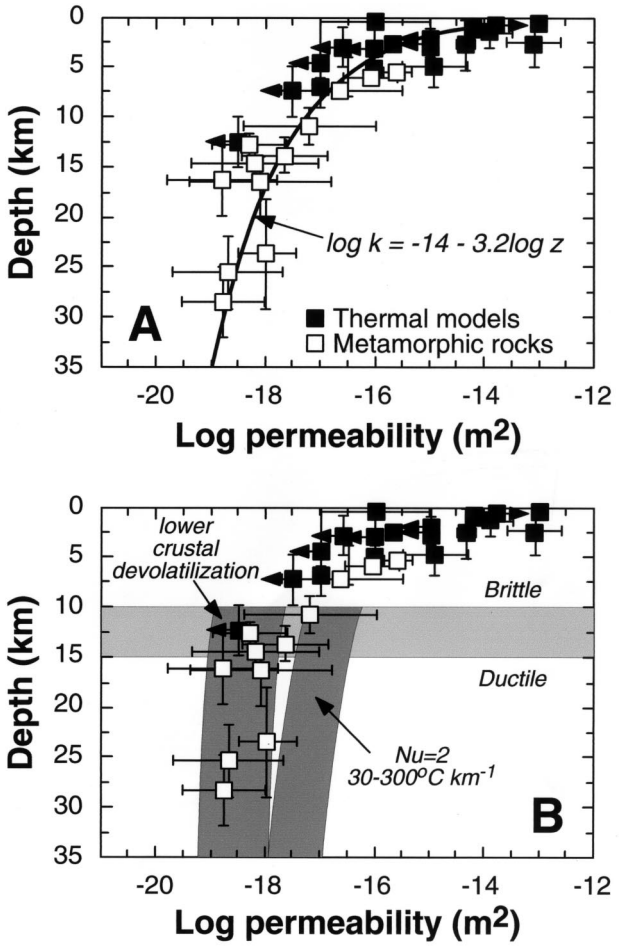

Figure 8. (a) Permeability as a function of depth in the continental crust, based on geothermal data (solid squares; Table 1), and metamorphic systems (open squares; Table 2). The solid line shows a logarithmic fit to all data. (b) Same data as in Figure 8a, but with curves added to illustrate process-limiting values.

The permeabilities in Figure 8a represent environments in which fluid flow was or is a consequence of tectonic or magmatic activity, such as sedimentary basin formation or prograde metamorphism. Lower permeabilities might be expected during metamorphism associated with cooling and decompression, or in the deep crust in stable cratons. Fault zones, which we have ignored in our analysis, may locally elevate permeability above the values in Figure 8a. With the exception of fault zones, the permeability-depth curve in Figure 8a likely represents the maximum attained at mid to lower crustal levels.

Figure 8b shows that the metamorphic-system permeability values at mid to lower crustal depths are consistent with values calculated assuming devolatilization of average crust at a flux of 10^{-8} kg (m^2-s)$^{-1}$, a geotherm of 30°C km^{-1}, and driving-force gradients of 20 and 1 MPa km^{-1}, reflecting vertical to subhorizontal flow. (The

arithmetic mean of the fluxes predicted by Table 2 is 1.4×10^{-8} kg $(m^2\text{-s})^{-1}$ for depths >10 km, as determined by dividing Q by Δt and assuming a fluid density of 750 kg m^{-3}.) The inferred metamorphic system permeability values are generally less than values required for a thermal Nusselt number of 2 for temperature gradients of 30°–300°C km^{-1}, which encompass expected ranges for crustal metamorphism, and a driving-force gradient of 1 MPa km^{-1}.

The relations in Figure 8b suggest an explanation for the narrow range of inferred metamorphic permeabilities. Active metamorphic systems need to be at least permeable enough to lose water under a lithostatic pressure gradient. This generally requires permeability of $\geq 10^{-19}$ m^2, depending on the rate of fluid production. At the same time, metamorphism is probably most efficient if the system is not permeable enough to lose significant heat by advection (i.e., $Nu \lesssim 2$). This generally requires $k \approx 10^{-18}$ to 10^{-17} under middle- to lower-crustal conditions. The near-coincidence of the values for dewatering and significant heat advection defines a narrow permeability range for hydrologically active metamorphism. The condition with $Nu \approx 2$ might reasonably be regarded as an optimum for such metamorphism because it defines the maximum transport of solute mass that is possible without advective cooling.

APPENDIX: PERMEABILITIES CONSTRAINED BY GEOTHERMAL DATA

A1. Sedimentary Basins

A1.1. Uinta basin. Geothermal observations in the Uinta basin, Utah, indicate moderately depressed heat flow in groundwater recharge areas and elevated heat flow in discharge areas [*Chapman et al*., 1984]. A numerical model of coupled groundwater flow and heat transport showed that these thermal observations could be matched by assigning a homogeneous, isotropic permeability of $\sim 5 \times 10^{-15}$ m^2 to the upper 3 km of the basin sediment, a value 2–3 orders of magnitude lower than the mean of in situ hydraulic test values for the same units [*Willett and Chapman*, 1987] (Table 1).

A1.2. North Slope basin. In the North Slope, Alaska, basin heat flow is depressed by groundwater downflow in the foothills of the Brooks Range and enhanced by upflow near the Arctic Ocean [*Deming et al*., 1992]. *Deming* [1993] treated the basin as homogeneous but anisotropic and showed that the thermal observations were well matched for particular ranges of horizontal and vertical permeability (Table 1). The thermally determined ranges are consistent with the results of in situ hydraulic measurements if one simply takes the arithmetic mean of the in situ values to represent k_x and the harmonic mean to represent k_z. (*Deming* [1993] also showed that the thermal observations were well matched with a heterogeneous permeability model that simply assigns in situ test values of permeability to each lithologic unit. But his approach made clear that the geothermal data themselves could be used to resolve only single values of k_x and k_z for the basin; any more complex model of permeability based only on the geothermal data would be overparameterized.)

A1.3. Arkoma basin and Rhine graben. Heat transport in the Arkoma basin of the North American midcontinent is conduction dominated, and *Lee et al*. [1996] used the *Domenico and Palciauskas* [1973] approach (equation (9)) to infer basin-scale permeability of $\leq 10^{-15}$ m^2. Heat transport in the northern Rhinegraben of southwest Germany is clearly affected by advection, and *Clauser* [1989] combined the *Bredehoeft and Papadopulos* [1965] approach (equation (5)) with numerical simulation to constrain basin-scale permeability in the narrow range of $3–6 \times 10^{-15}$ m^2.

A2. Other Environments

A2.1. California Coast Ranges. Investigation of heat flow in the vicinity of the San Andreas fault has led to a fairly strong consensus that the thermal regime of the California Coast Ranges is conductive [e.g., *Lachenbruch and Sass*, 1992]. Given the rugged topography of the Coast Ranges, which provides large driving-force gradients for groundwater flow, this implies that average upper crustal permeabilities of the (mainly) granitic and metamorphic rocks are less than 10^{-17} m^2, with near-surface permeabilities less than $\sim 10^{-15}$ m^2 [*Williams and Narasimhan*, 1989].

A2.2. Cascade Range. The Cascade Range volcanic arc of the Pacific Northwest is characterized by fairly high permeabilities in young, unaltered volcanic rocks and lower permeabilities in older volcanic rocks. In the broad highlands composed of young volcanic rocks (the High Cascades), the geothermal gradient is near zero owing to vigorous groundwater recharge. In older volcanic rocks, heat transport seems to be dominantly by conduction, with advection only in discrete zones. Replicating these observations in a numerical model required assigning permeabilities $\geq 10^{-14}$ m^2 in the youngest rocks and $\leq 10^{-16}$ m^2 in the oldest rocks [*Ingebritsen et al*., 1992].

A2.3. Hawaii. The island of Hawaii provides abundant geothermal and hydraulic data from volcanic rocks [*Ingebritsen and Scholl*, 1993]. The in situ permeability of the near-surface rocks is extremely high, averaging at least 10^{-10} m^2 [*Williams and Soroos*, 1973]. Hydrothermally altered rocks at greater depths have somewhat reduced permeability, and densely intruded and altered rocks at even greater depths are much less permeable (Table 1). Evidence for high-, moderate-, and low-permeability zones can be seen in the temperature profile from a National Science Foundation (NSF)–funded drill hole (Figure 9) located in Kilauea caldera just southwest of Halemaumau. Although this drill hole is believed to overlie Kilauea's magma chamber, the

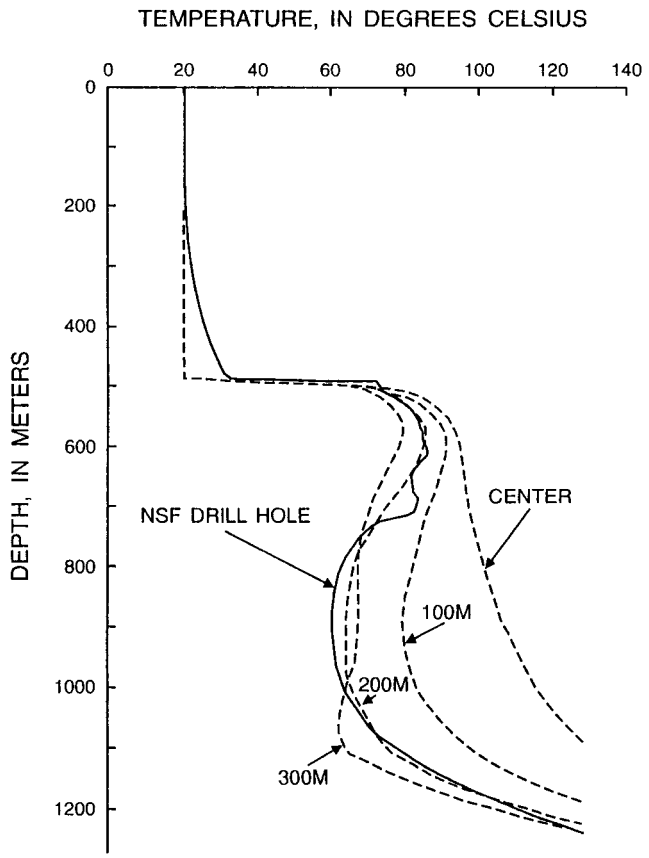

Figure 9. Temperatures from *Murray*'s [1974, Figure 17] numerical simulations (dashed lines) compared with the observed profile from the NSF drill hole (solid line) in Kilauea caldera. Distances (100 m, 200 m, 300 m) are relative to the center of a model with a horizontal half-cell dimension of 700 m. The upper boundary is at 500 m depth and is held constant at a temperature of 20°C (near surface ambient). The lower boundary is at 1900-m depth and maintained at 650°C. The 1200–1900 m depth interval is impermeable.

temperature profile is nearly isothermal to a depth of about 500 m because the high near-surface permeability allows copious groundwater recharge. Between 500- and 1200-m depth there are signs of free convection, which requires at least moderate permeability. Below 1200-m depth there is no sign of convective overturn despite a very high temperature gradient. The lack of convection below ~1-km depth despite high temperature gradients seems to be typical of wells in Kilauea's volcanic rift zones [*Kauahikaua*, 1993], and a Rayleigh number approach can be used to infer that permeability at such depths is generally less than 10^{-15} m^2, a value consistent with long-term flow test data from the HGP-A well in Kilauea's East Rift Zone ($k \approx 10^{-16}$ m^2) [*Ingebritsen and Scholl*, 1993].

A2.4. Jura overthrust. In the Aare Valley of north central Switzerland a positive, closed heat flow anomaly overlies the main Jura overthrust. The favored mechanism to explain the heat flow anomaly is upflow of deep fluids, a model that requires crystalline basement rock at depths of ~3–7 km to have vertical permeability in the range of 5×10^{-15} to 3×10^{-16} m^2 [*Griesser and Rybach*, 1989].

A2.5. Kola drill hole. A superdeep drill hole on the Kola Peninsula, Russia, penetrates crystalline rocks of the Fennoscandian shield to a depth of 12.3 km. Heat flow data from the hole show large (>twofold) variations with depth, an observation that can be explained in terms of topographically driven groundwater flow if the permeability of the upper 4 km of the crust is in the range of 10^{-15}–10^{-14} m^2 [*Kukkonen and Clauser*, 1994].

A2.6. KTB drill hole. The KTB superdeep drill hole penetrates 9.1 km of a gneiss-metabasite complex in northeast Bavaria and allowed measurement of in situ permeability at depths that amount to about one-third the thickness of the European continental crust. Modeling of the fluid flow and heat transport at the scale of the entire crust, constrained by the observed absence of thermally significant convection at depth, indicates permeabilities of $\leq 10^{-17}$ m^2 for large rock volumes [*Clauser et al.*, 1997]. The results of in situ (drawdown) tests indicate generally higher permeability values, of the order of 10^{-17}–10^{-15} m^2 above 4-km depth and 5×10^{-18} to 2×10^{-16} m^2 below [*Huenges et al.*, 1997].

ACKNOWLEDGMENTS. Barbara Bekins (U.S. Geological Survey) and Dennis Bird (Stanford University) provided thorough and constructive reviews of earlier versions of this manuscript, as did *Reviews of Geophysics* referees Jay Ague (Yale University) and Douglas Rumble (Carnegie Institute of Washington). The paper also benefited from the comments of an anonymous interdisciplinary referee and Editor Thomas Torgersen.

Thomas Torgersen was the Editor responsible for this paper. He thanks Jay Ague and Douglas Rumble for their technical reviews, and an anonymous referee for the cross-disciplinary review.

REFERENCES

Ague, J. J., Mass transfer during Barrovian metamorphism of pelites, south-central Connecticut, II, Channelized fluid flow and the growth of staurolite and kyanite, *Am. J. Sci.*, *294*, 1061–1134, 1994.

Ague, J. J., Deep crustal growth of quartz, kyanite and garnet into large-aperture, fluid-filled fractures, north-eastern Connecticut, USA, *J. Metamorph. Geol.*, *13*, 299–314, 1995.

Ague, J. J., Crustal mass transfer and index mineral growth in Barrow's garnet zone, northeast Scotland, *Geology*, *25*, 73–76, 1997.

Austrheim, H., Eclogitization of lower crustal granulites by fluid migration through shear zones, *Earth Planet. Sci. Lett.*, *81*, 221–232, 1987.

Austrheim, H., and A. K. Engvik, Fluid transport, deformation and metamorphism at depth in a collision zone in *Fluid Flow and Transport in Rocks: Mechanisms and Effects*, edited by B. Jamtveit and B. W. D. Yardley, pp. 123–137, Chapman and Hall, New York, 1997.

Auzerais, F. M., J. Dunsmuir, B. B. Ferreol, N. Martys, J. Olson, T. S. Ramakrishnan, D. H. Rothman, and L. M.

Schwartz, Transport in sandstone: A study based on three-dimensional microtomography, *Geophys. Res. Lett*., *23*, 705–708, 1996.

Baumgartner, L. P., and J. M. Ferry, A model for coupled fluid-flow and mixed-volatile mineral reactions with applications to regional metamorphism, *Contrib. Mineral. Petrol*., *106*, 273–285, 1991.

Baumgartner, L. P., and D. Rumble III, Transport of stable isotopes, I, Development of a kinetic continuum theory for stable isotope transport, *Contrib. Mineral. Petrol*., *98*, 417–430, 1988.

Baumgartner, L. P., M. L. Gerdes, M. A. Person, and G. T. Roselle, Porosity and permeability of carbonate rocks during contact metamorphism, in *Fluid Flow and Transport in Rocks: Mechanisms and Effects*, edited by B. Jamtveit and B. W. D. Yardley, pp. 83–98, Chapman and Hall, New York, 1997.

Bayuk, I. E., B. P. Belikov, L. I. Vernik, M. P. Volarovitch, Yu. I. Kuznetsov, G. E. Kuzmenkova, and N. N. Pavlova, Rock density, porosity, and permeability, in *The Superdeep Well of the Kola Peninsula*, edited by Ye. A. Kozlovsky, pp. 332–338, Springer-Verlag, New York, 1987.

Bear, J., *Dynamics of Fluids in Porous Media*, Am. Elsevier, New York, 1972.

Belitz, K., and J. D. Bredehoeft, Hydrodynamics of the Denver Basin: Explanation of subnormal fluid pressure, *AAPG Bull*., *72*, 1334–1359, 1988.

Bethke, C. M., and S. Marshak, Brine migrations across North America—The plate tectonics of groundwater, *Annu. Rev. Earth Planet. Sci*., *18*, 287–315, 1990.

Bickle, M. J., and J. Baker, Advective-diffusive transport of isotopic fronts: An example from Naxos, Greece, *Earth Planet. Sci. Lett*., *97*, 78–93, 1990.

Bickle, M. J., and D. McKenzie, The transport of heat and matter by fluids during metamorphism, *Contrib. Mineral. Petrol*., *95*, 384–392, 1987.

Blair, S. C., P. A. Gerge, and J. G. Berryman, Using two-point correlation functions to characterize microgeometry and estimate permeabilities of sandstones and porous glass, *J. Geophys. Res*., *101*, 20,359–20,375, 1996.

Bowers, J. R., D. M. Kerrick, and K. P. Furlong, Conduction model for the thermal evolution of the Cupsuptic aureole, Maine, *Am. J. Sci*., *290*, 644–665, 1990.

Brace, W. F., Permeability of crystalline and argillaceous rocks, *Int. J. Rock Mech. Min. Sci. Geomech. Abstr*., *17*, 241–251, 1980.

Brace, W. F., Permeability of crystalline rocks: New in situ measurements, *J. Geophys. Res*., *89*, 4327–4330, 1984.

Bredehoeft, J. D., and B. B. Hanshaw, On the maintenance of anomalous fluid pressures, I, Thick sedimentary sequences, *Geol. Soc. Am. Bull*., *79*, 1097–1106, 1968.

Bredehoeft, J. D., and I. S. Papadopolous, Rates of vertical groundwater movement estimated from the Earth's thermal profile, *Water Resour. Res*., *1*, 325–328, 1965.

Bredehoeft, J. D., R. G. Wolff, W. S. Keys, and E. Shuter, Hydraulic fracturing to determine the regional in situ stress, Piceance Basin, Colorado, *Geol. Soc. Am. Bull*., *87*, 250–258, 1976.

Brenan, J. M., Development and maintenance of metamorphic permeability: implications for fluid transport, in *Contact Metamorphism*, *Rev. Mineral*., vol. 26, edited by D. M. Kerrick, pp. 291–319, Mineral. Soc. of Am., Washington, D. C., 1991.

Burton, K. W., and R. K. O'Nions, High-resolution garnet chronometry and the rates of metamorphic processes, *Earth Planet. Sci. Lett*., *107*, 649–671, 1991.

Byerlee, J. D., Friction, overpressure, and fault normal compression, *Geophys. Res. Lett*., *17*, 2109–2203, 1990.

Byerlee, J. D., Model for episodic flow of high-pressure water in fault zones before earthquakes, *Geology*, *21*, 303–306, 1993.

Cartwright, I., The two-dimensional pattern of metamorphic fluid flow at Mary Kathleen, Australia: Fluid focusing, transverse dispersion, and implications for modelling fluid flow, *Am. Mineral*., *79*, 526–535, 1994.

Cartwright, I., and I. S. Buick, Formation of wollastonite marbles during late regional metamorphic channelled fluid flow in the upper calcsilicate unit of the Reynolds Range Group, central Australia, *J. Metamorph. Geol*., *13*, 397–417, 1995.

Cartwright, I., and N. H. S. Oliver, Direction of fluid flow during contact metamorphism around the Burstall Granite, Australia, *J. Geol. Soc. London*, *149*, 693–696, 1992.

Cartwright, I., and N. H. S. Oliver, Fluid flow during contact metamorphism at Mary Kathleen, Queensland, Australia, *J. Petrol*., *35*, 1493–1521, 1994.

Cartwright, I., and T. R. Weaver, Fluid-rock interaction between syenites and marbles at Stephen Cross Quarry, Quebec, Canada: Petrologic and stable isotope data, *Contrib. Mineral. Petrol*., *113*, 533–544, 1993.

Cartwright, I., J. Vry, and M. Sandiford, Changes in stable isotope ratios of metapelites and marbles during regional metamorphism, Mount Lofty Ranges, South Australia: Implications for crustal scale fluid flow, *Contrib. Mineral. Petrol*., *120*, 292–310, 1995.

Chapman, D. S., T. H. Keho, M. S. Bauer, and M. D. Picard, Heat flow in the Uinta basin determined from bottom hole temperature (BHT) data, *Geophysics*, *49*, 453–466, 1984.

Christensen, J. N., J. L. Rosenfeld, and D. J. DePaolo, Rates of tectonometamorphic processes from rubidium and strontium isotopes in garnet, *Science*, *224*, 1465–1469, 1989.

Christensen, J. N., J. Selverstone, J. L. Rosenfeld, and D. J. DePaolo, Correlation by Rb-Sr geochronology of garnet growth histories from different structural levels within the Tauern Window, Eastern Alps, *Contrib. Mineral. Petrol*., *118*, 1–12, 1994.

Clauser, C., Conductive and convective heat flow components in the Rheingraben and implications for the deep permeability distribution, in *Hydrological Regimes and Their Subsurface Thermal Effects*, *Geophys. Monogr. Ser*., vol. 47, edited by A. E. Beck, G. Garven, and L. Stegena, pp. 59–64, AGU, Washington, D. C., 1989.

Clauser, C., Permeability of crystalline rocks, *Eos Trans. AGU*, *73*, 233, 237, 1992.

Clauser, C., P. Giese, E. Huenges, T. Kohl, H. Lehmann, L. Rybach, J. Safanda, H. Wilhelm, K. Windloff, and G. Zoth, The thermal regime of the continental crust: Implications from the KTB, *J. Geophys. Res*., *102*, 18,417–18,441, 1997.

Connolly, J. A. D., Mid-crustal focused fluid movement: Thermal consequences and silica transport, in *Fluid Flow and Transport in Rocks*, edited by B. Jamtveit and B. W. D. Yardley, pp. 235–250, Chapman and Hall, New York, 1997a.

Connolly, J. A. D., Devolatilization-generated fluid pressure and deformation-propagated fluid flow during prograde regional metamorphism, *J. Geophys. Res*., *102*, 18,149–18,173, 1997b.

Connolly, J. A. D., and A. B. Thompson, Fluid and enthalpy production during regional metamorphism, *Contrib. Mineral. Petrol*., *102*, 347–366, 1989.

Cook, S. J., J. R. Bowman, and C. B. Forster, Contact metamorphism surrounding the Alta stock: Finite element model simulation of heat- and $^{18}O/^{16}O$ mass-transport during prograde metamorphism, *Am. J. Sci*., *297*, 1–55, 1997.

Coombs, D. S., Dehydration veins in diagenetic and very-low grade metamorphic rocks: Features of the crustal seismogenic zone and their significance to mineral facies, *J. Metamorph. Geol*., *11*, 389–399, 1993.

Cox, S. F., and M. A. Etheridge, Coupled grain-scale dilatency and mass transfer during deformation at high fluid pressures: Examples from Mount Lyell, Tasmania, *J. Struct. Geol*., *11*, 147–162, 1989.

Cox, S. F., and M. S. Paterson, Experimental dissolution-precipitation creep in quartz aggregates at high temperatures, *Geophys. Res. Lett*., *18*, 1401–1404, 1991.

Coyle, B. J., and M. D. Zoback, In situ permeability and fluid pressure measurements at ~2 km depth in the Cajon Pass research well, *Geophys. Res. Lett*., *15*, 1029–1032, 1988.

Davis, S. R., and J. M. Ferry, Fluid infiltration during contact metamorphism of interbedded marble and calc-silicate hornfels, Twin Lakes area, central Sierra Nevada, California, *J. Metamorph. Geol*., *11*, 71–88, 1993.

Deming, D., Regional permeability estimates from investigations of coupled heat and groundwater flow, North Slope of Alaska, *J. Geophys. Res*., *98*, 16,271–16,286, 1993.

Deming, D., J. H. Sass, A. H. Lachenbruch, and R. F. DeRito, Heat flow and subsurface temperature as evidence for basin-scale groundwater flow, *Geol. Soc. Am. Bull*., *104*, 528–542, 1992.

Dipple, G. M., and J. M. Ferry, Fluid flow and stable isotopic alteration in rocks at elevated temperatures with applications to metamorphism, *Geochim. Cosmochim. Acta*, *56*, 3539–3550, 1992.

Domenico, P. A., and V. V. Palciauskas, Theoretical analysis of forced convective heat transfer in regional groundwater flow, *Geol. Soc. Am. Bull*., *84*, 3803–3814, 1973.

Dudziak, K. H., and E. U. Frank, Messung der Viscositaet des Wassers bis 560° und 3500 Bar, *Ber Bunsen Ges. Physik Chem*., *70*, 1120–1128, 1966.

Dutrow, B., and D. Norton, Evolution of fluid pressure and fracture propagation during contact metamorphism, *J. Metamorph. Geol*., *13*, 677–686, 1995.

Ehrlich, R., E. L. Etris, D. Brumfield, L. P. Yuan, and S. J. Crabtree, Petrography and reservoir physics, III, Physical models for permeability and formation factor, *AAPG Bull*., *75*, 1579–1592, 1991.

Emmerman, S. H., D. L. Turcotte, and D. A. Spence, Transport of magma and hydrothermal solutions by laminar and turbulent fluid fracture, *Phys. Earth Planet. Inter*., *41*, 249–259, 1986.

Etheridge, M. A., Differential stress magnitudes during regional deformation and metamorphism: Upper bound imposed by tensile fracturing, *Geol. 11*, 231–234, 1983.

Etheridge, M. A., V. J. Wall, and R. H. Vernon, The role of the fluid phase during regional metamorphism and deformation, *J. Metamorph. Geol*., *1*, 205–226, 1983.

Etheridge, M. A., V. J. Wall, S. F. Cox, and R. H. Vernon, High fluid pressures during regional metamorphism and deformation: Implications for mass transport and deformation mechanisms, *J. Geophys. Res*., *89*, 4344–4358, 1984.

Ferry, J. M., Contact metamorphism of roof pendants at Hope Valley, Alpine County, California, USA, *Contrib. Mineral. Petrol*., *101*, 402–417, 1989.

Ferry, J. M., Regional metamorphism of the Waits River Formation, eastern Vermont: Delineation of a new type of giant metamorphic hydrothermal system, *J. Petrol*., *33*, 45–94, 1992.

Ferry, J. M., A historical review of metamorphic fluid flow, *J. Geophys. Res*., *99*, 15,487–15,498, 1994a.

Ferry, J. M., Overview of the petrologic record of fluid flow during regional metamorphism in northern New England, *Am. J. Sci*., *294*, 905–988, 1994b.

Ferry, J. M., S. S. Sorenson, and D. Rumble III, Structurally controlled fluid flow during contact metamorphism in the Ritter Range pendant, California, USA, *Contrib. Mineral. Petrol*., *130*, 358–378, 1998.

Finlayson, B. A., *Numerical Methods for Problems with Moving Fronts*, Ravenna Park, Seattle, Wash., 1992.

Fischer, G. J., and M. S. Paterson, Measurement of permeability and storage capacity in rocks during deformation at high temperature and pressure, in *Fault Mechanics and Transport Properties of Rocks*, edited by B. Evans and T. Wong, pp. 213–252, Academic, San Diego, Calif., 1992.

Fourcade, S., D. Marquer, and M. Javoy, $^{18}O/^{16}O$ variations and fluid circulation in a deep shear zone: The case of the Alpine ultramylonites from the Aar massif (Central Alps, Switzerland), *Chem. Geol*., *77*, 119–132, 1989.

Freeze, R. A., and J. A. Cherry, *Groundwater*, Prentice-Hall, Englewood Cliffs, N. J., 1979.

Fruh Green, G. L., Interdependence of deformation, fluid infiltration, and reaction progress recorded in eclogitic metagranitoids (Sesia zone, Western Alps), *J. Metamorph. Geol*., *12*, 327–343, 1994.

Fyfe, W. S., N. J. Price, and A. B. Thompson, *Fluids in the Earth's Crust*, Elsevier, New York, 1978.

Gangi, A. F., Variation of whole and fractured porous rock permeability with confining pressure, *Int. J. Rock Mech. Min. Sci. Geomech. Abstr*., *15*, 249–257, 1978.

Ganor, J., A. Matthews, and N. Paldor, Constraints on effective diffusivity during oxygen isotope exchange at a marble-schist contact, Sifnos (Cyclades), Greece, *Earth Planet. Sci. Lett*., *94*, 208–216, 1989.

Garven, G., and R. A. Freeze, Theoretical analysis of the role of groundwater flow in the genesis of stratabound ore deposits, 1, Mathematical and numerical model, *Am. J. Sci*., *284*, 1085–1124, 1984a.

Garven, G., and R. A. Freeze, Theoretical analysis of the role of groundwater flow in the genesis of stratabound ore deposits, 2, Quantitative results, *Am. J. Sci*., *284*, 1125–1174, 1984b.

Garven, S., S. Ge, M. A. Person, and D. A. Sverjensky, Genesis of stratabound ore deposits in the midcontinent basins of North America, 1, The role of regional groundwater flow, *Am. J. Sci*., *293*, 497–568, 1993.

Gavrilenko, P., and Y. Geugen, Fluid overpressures and pressure solution in the crust, *Tectonophysics*, *217*, 91–110, 1993.

Gelhar, L. W., C. Welty, and K. R. Rehfeldt, A critical review of data on field-scale dispersion in aquifers, *Water Resour. Res*., *28*, 1955–1974, 1992.

Gold, T., and S. Soter, Fluid ascent through the solid lithosphere and its relation to earthquakes, *Pure Appl. Geophys*., *122*, 492–530, 1985.

Griesser, J.-C., and L. Rybach, Numerical thermohydraulic modeling of deep groundwater circulation in crystalline basement: An example of calibration, in *Hydrological Regimes and Their Subsurface Thermal Effects*, *Geophys. Monogr. Ser*., vol. 47, edited by A. E. Beck, G. Garven, and L. Stegena, pp. 65–74, AGU, Washington, D. C., 1989.

Hanson, R. B., Effects of fluid production on fluid flow during regional and contact metamorphism, *J. Metamorph. Geol*., *10*, 87–97, 1992.

Hanson, R. B., The hydrodynamics of contact metamorphism, *Geol. Soc. Am. Bull*., *107*, 595–611, 1995.

Hanson, R. B., Hydrodynamics of regional metamorphism due to continental collision, *Econ. Geol*., *92*, 880–891, 1997.

Harley, S. L., and I. S. Buick, Wollastonite-scapolite assemblages as indicators of granulite pressure-temperature-fluid histories: The Rauer Group, East Antarctica, *J. Petrol*., *33*, 693–728, 1992.

Harley, S. L., and M. Santosh, Wollastonite at Nuliyam, Kerala, southern India: A reassessment of CO_2-infiltration and charnockite formation at a classic locality, *Contrib. Mineral. Petrol*., *120*, 83–94, 1995.

Harris, N. B. W., and M. J. Bickle, Advective fluid transport

during charnockite formation: An example from southern India, *Earth Planet. Sci. Lett*., *93*, 151–156, 1989.

Harris, N. R. W., D. H. Jackson, D. P. Mattey, M. Santosh, and J. Bartlett, Carbon-isotope constraints on fluid advection during contrasting examples of incipient charnockite formation, *J. Metamorph. Geol*., *11*, 833–842, 1993.

Hayba, D. O., and S. E. Ingebritsen, The computer model HYDROTHERM, A three-dimensional finite-difference model to simulate ground-water flow and heat transport in the temperature range of 0 to 1,200°C, *U.S. Geol. Surv. Water Resour. Invest. Rep*., *94-4045*, 1994.

Hayba, D. O., and S. E. Ingebritsen, Multiphase groundwater flow near cooling plutons, *J. Geophys. Res*., *102*, 12,235–12,252, 1997.

Holdaway, M. J., and J. W. Goodge, Rock pressure versus fluid pressure as a controlling influence on mineral stability: An example from New Mexico, *Am. Mineral*., *75*, 1043–1058, 1990.

Holness, M. B., Equilibrium dihedral angles in the system quartz-CO_2-H_2O-NaCl at 800°C and 1–15 kbar: The effects of pressure and fluid composition on the permeability of quartzites, *Earth Planet. Sci. Lett*., *114*, 171–184, 1992.

Holness, M. B., Temperature and pressure dependence of quartz-aqueous fluid dihedral angles: The control of adsorbed H_2O on permeability of quartzites, *Earth Planet. Sci. Lett*., *117*, 363–377, 1993.

Holness, M. B., Surface chemical controls on pore-fluid connectivity in texturally equilibrated materials, in *Fluid Flow and Transport in Rocks: Mechanisms and Effects*, edited by B. Jamtveit and B. W. D. Yardley, pp. 149–169, Chapman and Hall, New York, 1997.

Hubbert, M. K., The theory of ground-water motion, *J. Geol*., *48*, 785–944, 1940.

Hubbert, M. K., and W. W. Rubey, Role of fluid pressure in mechanics of overthrust faulting, I, Mechanics of fluid-filled porous solids and its application to overthrust faulting, *Geol. Soc. Am. Bull*., *70*, 115–166, 1959.

Hubbert, M. K., and D. G. Willis, Mechanics of hydraulic fracturing, *Trans. Am. Inst. Min*., *Metall. Pet. Eng*., *210*, 153–168, 1957.

Huenges, E., J. Erzinger, J. Kuck, B. Engeser, and W. Kessels, The permeable crust: Geohydraulic properties down to 9101 m depth, *J. Geophys. Res*., *102*, 18,255–18,265, 1997.

Ingebritsen, S. E., and D. O. Hayba, Fluid flow and heat transport near the critical point of H_2O, *Geophys. Res. Lett*., *21*, 2199–2203, 1994.

Ingebritsen, S. E., and W. E. Sanford, *Groundwater in Geologic Processes*, Cambridge Univ. Press, New York, 1998.

Ingebritsen, S. E., and M. A. Scholl, The hydrogeology of Kilauea volcano, *Geothermics*, *22*, 255–270, 1993.

Ingebritsen, S. E., D. R. Sherrod, and R. H. Mariner, Rates and patterns of groundwater flow in the Cascade Range volcanic arc, and the effect on subsurface temperatures, *J. Geophys. Res*., *97*, 4599–4627, 1992.

Irwin, W. P., and I. Barnes, Effect of geologic structure and metamorphic fluids on seismic behavior of the San Andreas fault system in central and northern California, *Geology*, *3*, 713–716, 1975.

Jacob, C. E., On the flow of water in an elastic artesian aquifer, *Eos Trans. AGU*, *21*, 574–586, 1940.

Jamtveit, B., K. Bucher-Nurminen, and H. Austrheim, Fluid controlled eclogitization of granulites in deep crustal shear zones, Bergen Arcs, western Norway, *Contrib. Mineral. Petrol*., *104*, 184–193, 1990.

Jessop, A. M., M. A. Hobart, and J. G. Schlater, The world heat flow data collection—1975, *Geotherm. Ser*., vol. 5, Geother. Serv. of Can., Energy, Mines, and Resour. Can., Ottawa, Ont., 1976.

Kauahikaua, J., Geophysical characteristics of the hydrothermal systems of Kilauea volcano, Hawai'i, *Geothermics*, *22*, 271–299, 1993.

Ko, S.-C., D. L. Olgaard, and T.-F. Wong, Generation and maintenance of pore pressure excess in a dehydrating system, 1, Experimental and microstructural observation, *J. Geophys. Res*., *102*, 825–839, 1997.

Kukkonen, I. T., and C. Clauser, Simulation of heat transfer at the Kola deep-hole site: Implications for advection, heat refraction, and palaeoclimatic effects, *Geophys. J. Int*., *116*, 409–420, 1994.

Lachenbruch, A. H., and J. H. Sass, Heat flow from Cajon Pass, fault strength, and tectonic implications, *J. Geophys. Res*., *97*, 4995–5015, 1992.

Lee, Y., D. Deming, and K. F. Chen, Heat flow and heat production in the Arkoma basin and Oklahoma platform, southeastern Oklahoma, *J. Geophys. Res*., *101*, 25,387–25,401, 1996.

Léger, A., and J. M. Ferry, Fluid infiltration and regional metamorphism of the Waits River Formation, north-east Vermont, USA, *J. Metamorph. Geol*., *11*, 3–29, 1993.

Lowell, R. P., P. Van Cappellen, and L. N. Germanovich, Silica precipitation in fractures and the evolution of permeability in hydrothermal upflow zones, *Science*, *260*, 192–194, 1993.

Lowell, R. P., P. A. Rona, and R. P. Von Herzen, Seafloor hydrothermal systems, *J. Geophys. Res*., *100*, 327–352, 1995.

Maasland, M., Soil anisotropy and soil drainage, in *Drainage of Agricultural Lands*, edited by J. N. Maddock, pp. 216–285, Am. Soc. of Agron., Madison, Wis., 1957.

Manning, C. E., and D. K. Bird, Porosity evolution and fluid flow in the basalts of the Skaergaard magma-hydrothermal system, east Greenland, *Am. J. Sci*., *291*, 201–257, 1991.

Manning, C. E., and D. K. Bird, Porosity, permeability, and basalt metamorphism, in *Low-Grade Metamorphism of Mafic Rocks*, edited by P. Schiffman and W. H. Day, *Spec. Pap. Geol. Soc. Am*., *296*, 123–140, 1995.

Manning, C. E., S. E. Ingebritsen, and D. K. Bird, Missing mineral zones in contact metamorphosed basalts, *Am. J. Sci*., *293*, 894–938, 1993.

Mattey, D., D. H. Jackson, N. B. W. Harris, and S. Kelley, Isotopic constraints on fluid infiltration from an eclogite facies shear zone, Holseney, Norway, *J. Metamorph. Geol*., *12*, 311–325, 1994.

Mitchell, J. K., *Fundamentals of Soil Behavior*, 2nd ed., John Wiley, New York, 1993.

Morrow, C. A., and J. Byerlee, Permeability of rock samples from Cajon Pass, California, *Geophys. Res. Lett*., *15*, 1033–1037, 1988.

Morrow, C. A., and D. A. Lockner, Permeability differences between surface-derived and deep drillhole core samples, *Geophys. Res. Lett*., *21*, 2151–2154, 1994.

Morrow, C. A., D. Lockner, S. Hickman, M. Rusanov, and T. Rockel, Effects of lithology and depth on the permeability of core samples from the Kola and KTB drill holes, *J. Geophys. Res*., *99*, 7263–7274, 1994.

Mowers, T. T., and D. A. Budd, Quantification of porosity and permeability reduction due to calcite cementation using computer-assisted petrographic image analysis techniques, *AAPG Bull*., *80*, 309–322, 1996.

Murray, J. C., The geothermal system at Kilauea volcano, Hawaii, Ph.D. thesis, Colo. Sch. of Mines, Golden, 1974.

Nabelek, P. I., T. C. Labotka, J. R. O'Neil, and J. J. Papike, Contrasting fluid/rock interaction between the Notch Peak granitic intrusion and argillites and limestones in western Utah: Evidence from stable isotopes and phase assemblages, *Contrib. Mineral. Petrol*., *86*, 25–34, 1984.

Nakashima, Y., Buoyancy-driven propagation of an isolated fluid-filled crack in rock: Implication for fluid transport in metamorphism, *Contrib. Mineral. Petrol*., *114*, 289–295, 1993.

Nakashima, Y., Transport model of buoyant metamorphic fluid by hydrofracturing in leaky rock, *J. Metamorph. Geol*., *13*, 727–736, 1995.
Neglia, S., Migration of fluids in sedimentary basins, *AAPG Bull*., *63*, 573–597, 1979.
Neuzil, C. E., How permeable are clays and shales?, *Water Resour. Res*., *30*, 145–150, 1994.
Neuzil, C. E., Abnormal pressures as hydrodynamic phenomena, *Am. J. Sci*., *295*, 742–786, 1995.
Newton, R. C., Fluids and shear zones in the deep crust, *Tectonophysics*, *182*, 21–37, 1990.
Newton, R. C., J. V. Smith, and B. F. Windley, Carbonic metamorphism, granulites and crustal growth, *Nature*, *288*, 45–50, 1980.
Nishiyama, T., Kinetics of hydrofracturing and metamorphic veining, *Geology*, *17*, 1068–1071, 1989.
Norton, D., Pore fluid pressure near magma chambers, in *The Role of Fluids in Crustal Processes*, edited by J. D. Bredehoeft and D. Norton, pp. 42–49, Natl. Acad. Press, Washington, D. C., 1990.
Norton, D., and L. M. Cathles, Thermal aspects of ore deposition, in *Geochemistry of Hydrothermal Ore Deposits*, edited by H. L. Barnes, pp. 611–631, John Wiley, New York, 1979.
Norton, D., and J. E. Knight, Transport phenomena in hydrothermal systems: Cooling plutons, *Am. J. Sci*., *277*, 937–981, 1977.
Norton, D., and H. P. Taylor Jr., Quantitative simulation of the hydrothermal systems of crystallizing magmas on the basis of transport theory and oxygen isotope data: An analysis of the Skaergaard intrusion, *J. Petrol*., *20*, 421–486, 1979.
Norton, D., H. P. Taylor Jr., and D. K. Bird, The geometry and high-temperature brittle deformation of the Skaergaard intrusion, *J. Geophys. Res*., *89*, 10,178–10,192, 1984.
Nur, A., and J. Walder, Time-dependent permeability of the Earth's crust, in *The Role of Fluids in Crustal Processes*, edited by J. D. Bredehoeft and D. Norton, pp. 113–127, Natl. Acad. Press, Washington, D. C., 1990.
Oliver, N. H. S., Review and classification of structural controls on fluid flow during regional metamorphism, *J. Metamorph. Geol*., *14*, 477–492, 1996.
Palciauskas, V. V., and P. A. Domenico, Characterization of drained and undrained response of thermally loaded repository rocks, *Water Resour. Res*., *18*, 281–290, 1982.
Person, M. A., D. Toupin, and P. Eadington, One-dimensional models of groundwater flow, sediment thermal history, and petroleum generation within continental rift basins, *Basin Res*., *7*, 81–96, 1995.
Raleigh, C. B., J. H. Healy, and J. D. Bredehoeft, An experiment in earthquake control at Rangely, Colorado, *Science*, *191*, 1230–1236, 1976.
Rice, J. R., Fault stress states, pore pressure distributions, and the weakness of the San Andreas fault, in *Fault Mechanics and Transport Properties of Rocks*, edited by B. Evans and T.-F. Wong, pp. 475–503, Academic, San Diego, Calif., 1992.
Rojstaczer, S. A., and S. Wolf, Permeability changes associated with large earthquakes: An example from Loma Prieta, California, 10/17/89, *Geology*, *20*, 211–214, 1992.
Rosenberg, N. D., and F. J. Spera, Role of anisotropic and/or layered permeability in hydrothermal convection, *Geophys. Res. Lett*., *17*, 235–238, 1990.
Rubey, W. W., and M. K. Hubbert, Role of fluid pressures in mechanics of overthrust faulting, II, Overthrust belt in geosynclinal area of western Wyoming in light of fluid-pressure hypothesis, *Geol. Soc. Am. Bull*., *70*, 167–206, 1959.
Rumble, D., III, Evidences of fluid flow during regional metamorphism, *Eur. J. Mineral*., *1*, 731–737, 1989.
Rumble, D., III, Water circulation in metamorphism, *J. Geophys. Res*., *99*, 15,499–15,502, 1994.
Rumble, D., III, and F. S. Spear, Oxygen isotope equilibration and permeability enhancement during regional metamorphism, *J. Geol. Soc. London*, *140*, 619–628, 1983.
Rutter, E. H., and K. H. Brodie, Mechanistic interactions between deformation and metamorphism, *Geol. J*., *30*, 227–240, 1995.
Sanford, W. E., and L. F. Konikow, Simulation of calcite dissolution and porosity changes in salt water mixing zones in coastal aquifers, *Water Resour. Res*., *25*, 655–667, 1989.
Sardini, P., B. Ledesert, and G. Touchard, Quantification of microscopic porous networks by image analysis and measurements of permeability in the Soultz-sous-Forets granite (Alsace, France), in *Fluid Flow and Transport in Rocks: Mechanisms and Effects*, edited by B. Jamtveit and B. W. D. Yardley, pp. 171–189, Chapman and Hall, New York, 1997.
Sharp, J. M., Jr., and P. A. Domenico, Energy transport in thick sequences of compacting sediment, *Geol. Soc. Am. Bull*., *87*, 390–400, 1976.
Skelton, A. D. L., The timing and direction of metamorphic fluid flow in Vermont, *Contrib. Mineral. Petrol*., *125*, 75–84, 1996.
Skelton, A. D. L., C. M. Graham, and M. J. Bickle, Lithological and structural controls on regional 3-D fluid flow patterns during greenschist facies metamorphism of the Dalradian of the SW Scottish Highlands, *J. Petrol*., *36*, 563–586, 1995.
Smith, L., and D. S. Chapman, On the thermal effects of groundwater flow, 1, Regional scale systems, *J. Geophys. Res*., *88*, 593–608, 1983.
Smoluchowski, M. S., Some remarks on the mechanics of overthrusts, *Geol. Mag*., *56*, 12–17, 1909.
Snow, D. T., The frequency and apertures of fractures in rock, *Int. J. Rock Mech. Min. Sci*., *7*, 23–40, 1970.
Spanne, P., J. F. Thovert, C. J. Jacquin, W. B. Lindquist, K. W. Jones, and P. M. Adler, Synchrotron computed microtomography of porous media: Topology and transport, *Phys. Rev. Lett*., *73*, 2001–2004, 1994.
Stallman, R. W., Notes on the use of temperature data for computing ground-water velocity, in *Sixth Assembly on Hydraulics*, pp. 1–7, Soc. Hydrotech. de France, Paris, 1960. (Reprinted in Methods of collecting and interpreting ground-water data, edited by R. Bentall, *U.S. Geol. Surv. Water Supply Pap*., *1544-H*, 36–46, 1963.)
Stober, I., Researchers study conductivity of crystalline rock in proposed radioactive waste site, *Eos Trans. Am. Geophys. Union 77*, 93–94, 1996.
Swartzendruber, D., Non-Darcy flow behavior in liquid-saturated porous media, *J. Geophys. Res*., *67*, 5205–5213, 1962.
Taylor, H. P., Jr., Oxygen and hydrogen isotope constraints on the deep circulation of surface waters into zones of hydrothermal metamorphism and melting, in *The Role of Fluids in Crustal Processes*, edited by J. D. Bredehoeft and D. Norton, pp. 72–95, Natl. Acad. Press, Washington, D. C., 1990.
Taylor, H. P., Jr., and R. W. Forester, An oxygen isotope study of the Skaergaard intrusion and its country rocks: A description of a 55-m.y. old fossil hydrothermal system, *J. Petrol*., *20*, 355–419, 1979.
Thompson, A. B., Fluid-absent metamorphism, *J. Geol. Soc. London*, *140*, 533–547, 1983.
Titley, S. R., Evolution and style of fracture permeability in intrusion-centered hydrothermal systems, in *The Role of Fluids in Crustal Processes*, edited by J. D. Bredehoeft and D. Norton, pp. 50–63, Natl. Acad. Press, Washington, D. C., 1990.
Vance, D., and R. K. O'Nions, Prograde and retrograde thermal histories from the central Swiss Alps, *Earth Planet. Sci. Lett*., *114*, 113–129, 1992.
van Haren, J. L. M., J. J. Ague, and D. M. Rye, Oxygen isotope

record of fluid infiltration and mass transfer during regional metamorphism of pelitic schist, south-central Connecticut, USA, *Geochim. Cosmochim. Acta*, *60*, 3487–3504, 1996.

Walder, J., and A. Nur, Porosity reduction and crustal pore pressure development, *J. Geophys. Res*., *89*, 11,539–11,548, 1984.

Walther, J. V., Fluid-rock reactions during metamorphism at mid-crustal conditions, *J. Geol*., *102*, 559–570, 1994.

Walther, J. V., and P. M. Orville, Volatile production and transport in regional metamorphism, *Contrib. Mineral. Petrol*., *79*, 252–257, 1982.

Watson, E. B., and J. M. Brenan, Fluids in the lithosphere, 1, Experimentally determined wetting characteristics of CO_2-H_2O fluids and their implications for fluid transport, host-rock physical properties, and fluid inclusion formation, *Earth Planet. Sci. Lett*., *85*, 497–515, 1987.

Willet, S. D., and D. S. Chapman, Temperatures, fluid flow, and the thermal history of the Uinta basin, in *Migration of Hydrocarbons in Sedimentary Basins*, edited by B. Doligez, pp. 533–551, Technip, Paris, 1987.

Willet, S. D., and D. S. Chapman, Temperatures, fluid flow, and heat transfer in the Uinta basin, in *Hydrological Regimes and Their Subsurface Thermal Effects*, *Geophys. Monogr. Ser*., vol. 47, edited by A. E. Beck, G. Garven, and L. Stegena, pp. 29–33, AGU, Washington, D. C., 1989.

Williams, C. F., and T. N. Narasimhan, Hydrogeologic constraints on heat flow along the San Andreas fault: A testing of hypotheses, *Earth Planet. Sci. Lett*., *92*, 131–143, 1989.

Williams, J. A., and R. L. Soroos, Evaluation of methods of pumping test analysis for application to Hawaiian aquifers, *Tech. Rep. 20*, 159 pp., Water Resour. Res. Cent., Univ. of Hawaii, Honolulu, 1973.

Winograd, I. J., Hydrogeology of ash-flow tuff: A preliminary statement, *Water Resour. Res*., *7*, 994–1006, 1971.

Wong, T.-F., S.-C. Ko, and D. L. Olgaard, Generation and maintenance of pore pressure excess in a dehydrating system, 2, Theoretical analysis, *J. Geophys. Res*., *102*, 841–852, 1997.

Young, E. D., and D. Rumble III, The origin of correlated variations in in-situ $^{18}O/^{16}O$ and elemental concentrations in metamorphic garnet from southeastern Vermont, *Geochim. Cosmochim. Acta*, *57*, 2585–2597, 1993.

Zoback, M. L., and M. D. Zoback, Crustal stress and intraplate deformation, *Geowissenschaften*, *15*, 116–123, 1997.

S. E. Ingebritsen, Mail Stop 439, U.S. Geological Survey, 345 Middlefield Road, Menlo Park, CA 94025.

C. E. Manning, Department of Earth and Space Science, University of California, Los Angeles, CA 90095.